Structural design solutions for prefabricated timber façade systems

Sven Demolder

Supervisors: Anthony Tetaert, Gerhard Fink

Master's dissertation submitted in order to obtain the academic degree of
Master of Science in de industriële wetenschappen: bouwkunde

Department of Structural Engineering
Chair: Prof. dr. ir. Luc Taerwe
Faculty of Engineering and Architecture
Academic year 2016-2017

GHENT UNIVERSITY

Structural design solutions for prefabricated timber façade systems

Sven Demolder

Supervisors: Anthony Tetaert, Gerhard Fink

Master's dissertation submitted in order to obtain the academic degree of
Master of Science in de industriële wetenschappen: bouwkunde

Department of Structural Engineering
Chair: Prof. dr. ir. Luc Taerwe
Faculty of Engineering and Architecture
Academic year 2016-2017

GHENT UNIVERSITY

Foreword

This master dissertation is the result of an interesting study, performed during my Erasmus+ exchange period at Aalto University, Finland. I would like to use this opportunity to thank a few people without whom this project wouldn't be possible.

First of all, I would like to thank my supervisor at Aalto University, Gerhard Fink. He was always available for questions and was always very helpful for giving feedback and support during the project. It goes without saying that I am very grateful that he was my supervisor for this project.

I would like to express my gratitude towards my supervisor at Ghent University, Anthony Tetaert. He gave me the opportunity to take part in the Erasmus+ project.

I would also like to take some time to thank professor Xiaoshu Lu. She gave me some insightful tips regarding building physics and thermal comfort and was also the one advising me to use Comsol Multiphysics.

For their help at the start of my exchange period in Finland, I would like to thank Hannele Pietola and Kristiina Hallaselkä.

Last but not least, I would like to thank all my friends and family for their support. It wouldn't be possible to complete this thesis without them. Thank you all.

June 2017,

Sven Demolder

Abstract

Structural design solutions for prefabricated timber façade systems

Sven Demolder

Supervisors: Anthony Tetaert, Gerhard Fink

Master's dissertation submitted in order to obtain the academic degree of
Master of Science in de industriële wetenschappen: bouwkunde

Department of Structural Engineering
Chair: Prof. dr. ir. Luc Taerwe
Faculty of Engineering and Architecture
Academic year 2016-2017

Although prefabrication of timber façade elements is gaining in popularity, most of the existing research focuses on timber frame systems. Cross-laminated timber, however, is a very interesting material to work with and could be an excellent solution for prefabricated façade systems. The present work investigates the connections of prefabricated façade systems with a CLT substructure. More specifically, this study focusses on the effect of large-diameter-connections on heat transfer and thermal bridging. The dissertation consists of two parts. In the first part, the required number of screws to connect cladding elements to a CLT structure is calculated based on Eurocodes and design guides. During the second part of the research, several simplified models are simulated with Comsol Multiphysics to calculate the thermal transmittance and internal surface temperatures of the external wall. The main findings from this study claim that the connections have little effect on thermal transmittance. Therefore, it could be possible to connect cladding elements with a smaller amount of large-diameter-connections, which could be interesting for a replaceable cladding system.

Keywords: prefabricated façade systems, CLT, connections, Comsol, heat transfer, thermal bridge

Extended abstract

Structural design solutions for prefabricated timber façade systems

Sven Demolder

Supervisors: Anthony Tetaert, Gerhard Fink

***Abstract* – The present paper investigates the connections of prefabricated façade systems with a CLT substructure. More specifically, this study focusses on the effect of large-diameter-connections on heat transfer and thermal bridging. In the first part of the research, the required number of screws to connect the cladding to the CLT is calculated. In the second part, several models are simulated with Comsol Multiphysics to calculate the thermal transmittance and internal surface temperatures of the external wall. The main findings from this study claim that the connections have little effect on thermal transmittance. Therefore, it should be possible to connect cladding elements with a smaller amount of large-diameter connections.**

Keywords: *prefabricated façade systems, CLT, connections, Comsol, heat transfer, thermal bridge*

1 Introduction

Although prefabrication of timber façade elements is gaining in popularity, most of the existing research focuses on timber frame systems. However, cross-laminated timber (CLT) is a very interesting material to work with and could be an excellent solution for prefabricated façade systems.

Very recently, Gasparri et al. investigated the different possibilities of prefabricated façade elements for tall CLT buildings [1][2]. They compared an existing CLT construction method with a prefabricated CLT system. The prefabricated system provided a cost reduction and showed to be much faster [1]. Gasparri et al. designed and compared different setups for such a prefabricated CLT façade system [2]. Figure 1 shows a vertical cross-section of a horizontal floor/wall joint. The cladding in this example is made of vertically oriented fir wood planks, fixed through screws on two wood mullions. The insulation is double density rock wool, pressed between a timber frame. The timber frame has a *projected part* at the bottom of the panel that is reinforced with OSB. The joint between the two panels is filled with low density rock wool insulation. A metal flashing/fire barrier is installed in the joint, fixed in the CLT floor slab.

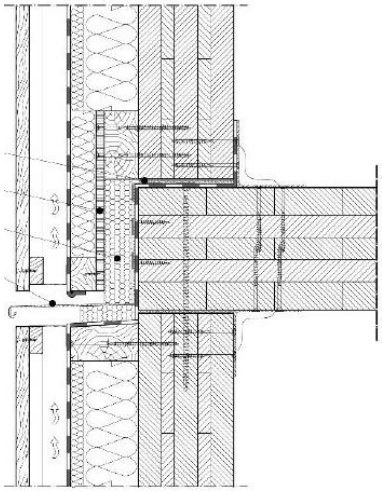

Figure 1 – Horizontal joint façade system Gasparri et al. [2]

2 Aim and scope

Most of the buildings that were built from ’50 to ’80 don’t meet the current energy regulations anymore. A lot of these old building need to have their façade renovated [3]. Since it’s difficult to predict the energy requirements in the future, it could be interesting to look into façade systems that are easily replaceable. This way, the façade insulation could be easily replaced or increased. Another advantage of replaceable façade systems could be the added value from an architectural point of view.

The challenge for this kind of replaceable cladding type are the connections to the load-bearing substructure. The first solution that comes to mind, is to use less connections but with a larger diameter. This raises of course the question of the effect on heat transfer through these connections.

This master's dissertation has therefore investigated the consequences of using these large-diameter-connections. In the first part of the research the minimum required number of screws to connect the cladding system to the CLT wall is calculated. In the second part of the research several models are simulated with Comsol Multiphysics.

3 Connection design

The defining loads acting on the façade connection are the permanent load of the cladding element G_d and the wind suction on the façade W_d. The connection will be subjected to withdrawal because of the wind suction and to shear because of the self-weight of the cladding. The withdrawal resistance $R_{ax,d}$ and shear resistance $R_{v,d}$ are calculated according to the CLT design guide, provided by proHolz [4] and according to EN 1995-1-1 [5].

The required number of screws is then calculated by dividing the loads by the connection capacity and taking the maximum of the two values:

$$n_{req} = \max\left(\frac{G_d}{R_{v,d}}; \frac{W_d}{R_{ax,d}}\right) \qquad (1)$$

The only variable parameters for this calculation are the area A of the cladding element, the screw diameter D and the penetration depth of the connection in the CLT, which depends on the CLT thickness. The results for the required number of screws is shown in Figure 2 and Figure 3. Screws with a diameter of 16 mm are only possible for CLT160 because the CLT element must be at least 10 times the screw diameter.

The results for n_{req} must always be round up to an even number. The code prescribes at least 2 screws per connection, so n_{req} is either 2, 4, 8 ...

From the results can be concluded that most of the times 2 screws will suffice as long as the dimensions of the cladding element don't get too large.

4 Modelling and simulation

Three different model types have been simulated. The design of the models is based on the CLT façade system of Gasparri et al. [2]. The first model type is a simplified 1 x 1 m² model with the connection through the timber frame and mullions in the centre. The model type varies for CLT thickness (CLT140, CLT160) and for screw diameter (D0, D8, D10, D12, D16). The second type is the same simplified model, but this time for a panel of 3x4 m² with two connections on the sides.

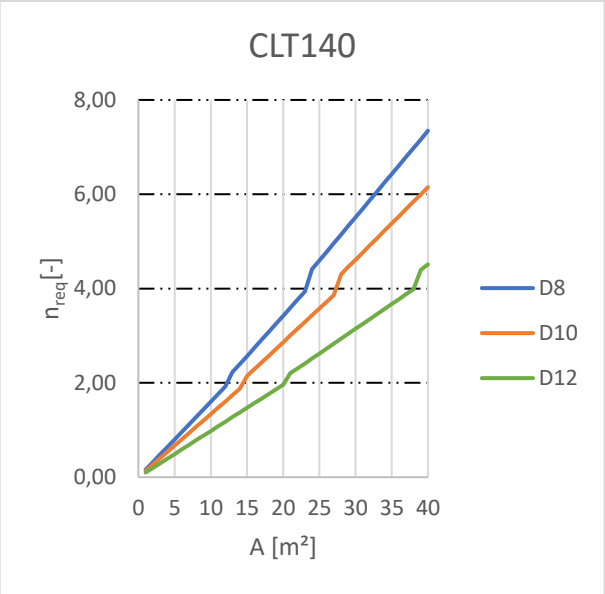

Figure 2 – Required number of screws for CLT140

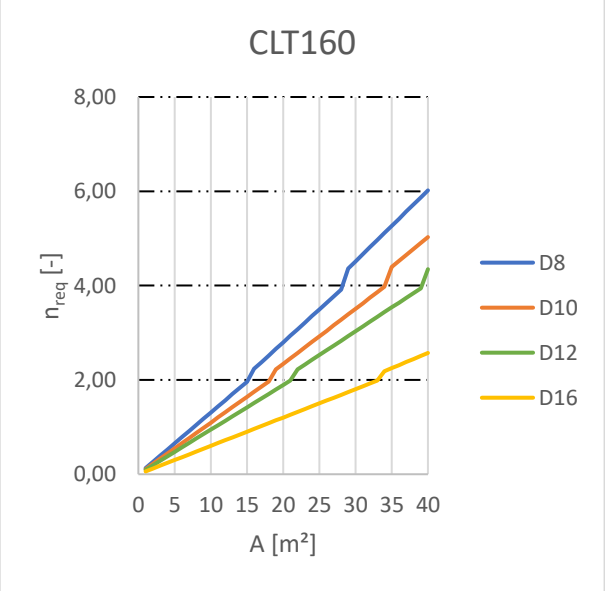

Figure 3 – Required number of screws for CLT160

The third model type is a more accurate representation of a floor/wall joint with a steel fire barrier between upper and lower floor level and with connections close to the edge of the elements. The floor/wall joint model had different configurations according to the presence of the steel barrier and the position of the connections.

The boundary conditions of all models were the same: $T_i = +20°C$ and $T_e = -20°C$.

A. Heat flow visualisation

Comsol provided different ways to visualize the heat flow through the façade. Figure 4 shows the temperature distribution near a connection. It is clearly visible that the temperature distribution is *deflected* in the surrounding area of the screw.

It was found that a temperature curve along the axis of the connection is the best visualisation method to compare the different models with each other (Figure 5). It appears that the main influential parameter between the models is rather the remaining thickness of the CLT after the connection point, than the anchor length of the screw.

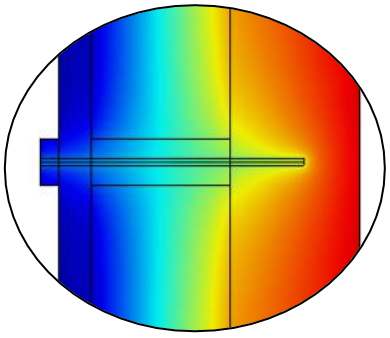

Figure 4 – Temperature distribution around the connection

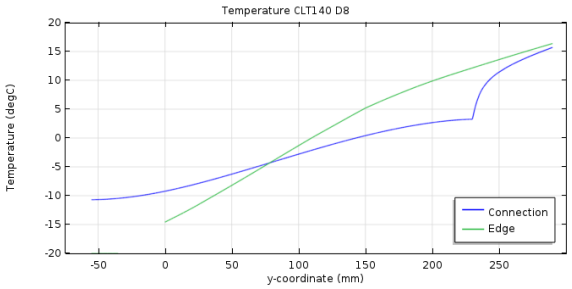

Figure 5 – Temperature curve along connection axis

B. Thermal transmittance

The thermal performances of a façade are usually evaluated by its thermal transmittance, better known as its U-value [W/m^{2}K]. However, it's not possible to let Comsol calculate the U-value, but it is possible to obtain the heat flux and then calculate the U-value with this formula:

$$U = \frac{\phi}{A.\Delta T} \qquad (2)$$

The results of these calculations showed that the thicker CLT160 panels performed better. But the differences appear on a level of 10^{-3} W/m^{2}K, so the difference between them is rather small and negligible. Since the U-value is a global parameter, it was decided to look at a local parameter: the internal surface temperature.

C. Internal surface temperature

The maximum and minimum internal surface temperature are calculated for each model and plotted together with a temperature distribution on the internal surface. Figure 6 shows the temperature distribution of the CLT140-D8 model.

The difference between the 1 x 1 m^2 models and the 3 x 4 m^2 models is negligible. But the difference among the floor/wall joint models is rather large. Apparently, the steel fire barrier has a big influence on the heat transfer of the model, even more than the effect of the connections.

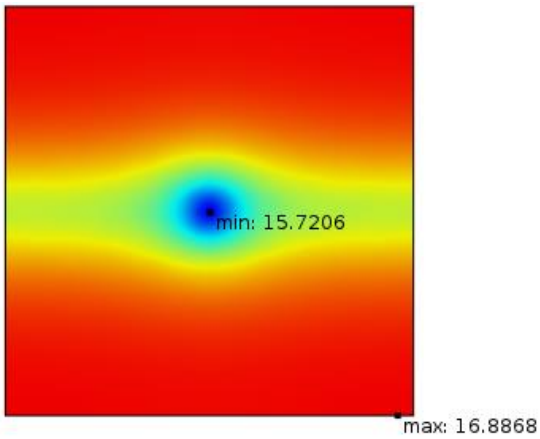

Figure 6 – Internal surface temperature distribution

5 Discussion of the results

Since the connections had very little influence on the thermal transmittance, the consequences for surface condensation risk or local thermal discomfort have been investigated.

The condensation risk is checked with the temperature factor f_{Rsi}, according to EN ISO 13788:2012 [6]:

$$f_{Rsi} = \frac{T_{si} - T_e}{T_i - T_e} \qquad (3)$$

All models have a temperature factor above 0.70, which is OK for both the Belgian and Finnish regulations [7].

Local discomfort is checked according to EN ISO 7730:2005 [8]. The two defining factors for local discomfort in this case are the vertical temperature difference and the radiant asymmetry. The percentage dissatisfied for local discomfort by radiant asymmetry (PD_r) is OK for all models. But because of the percentage dissatisfied for vertical temperature difference (PD_v), some models are categorized in lower comfort categories. This is especially the case with the floor/wall joints, but the cause of this is rather the steel barrier than the connections.

6 Conclusion

The presence of connections has very little influence on the thermal transmittance of the façade. They do have a certain effect on the internal surface temperature, but this effect is equally important as the horizontal floor/wall joint. The only factor that needs attention is the local thermal discomfort caused by the vertical temperature difference.

So, large-diameter-connections have very little effect on the heat transfer of the façade. This means that it could be possible to connect cladding elements to a CLT structure with fewer connections, resulting in higher construction speed and perhaps even the possibility to create a replaceable cladding system.

References

[1] Gasparri, E., Lucchini, A., Mantegazza, G., & Mazzucchelli, E. S. (2015). Construction management for tall CLT buildings: From partial to total prefabrication of façade elements. *Wood Material Science & Engineering, 10*(3), 256-275.

[2] Gasparri, E., Giunta, G., Mazzucchelli, E. S., & Lucchini, A. (2016). *Prefabricated CLT façade systems for fast-track construction and quality assurance.* Paper presented at the proceedings of World Conference on Timber Engineering, Wien, Austria.

[3] Maroy, K., Van Den Bossche, N., Steeman, M., De Corte, W., & Janssens, A. (2016). *Potential of existing prefabricated components for sustainable renovation of buildings.* Paper presented at the CESB16: Central Europe towards Sustainable Building 2016.

[4] proHolz. (2014). Cross-Laminated Timber Structural Design - Basic design and engineering principles according to Eurocode. Vienna: proHolz Austria.

[5] EN 1995-1-1. (2004). *Eurocode 5: Design of timber structures - Part 1-1: General - Common rules and rules for buildings*. Brussels: European committee for standardization.

[6] EN ISO 13788. (2012). *Hygrothermal performance of building components and building elements - Internal surface temperature to avoid critical surface humidity and interstitial condensation - Calculation methods*. Brussels: European committee for standardization.

[7] Kalamees, T. (2006). *Critical values for the temperature factor to assess thermal bridges.* Paper presented at the Proceedings of the Estonian Academy of Sciences.

[8] EN ISO 7730. (2005). *Ergonomics of the thermal environment - Analytical determination and interpretation of thermal comfort using calculation of the PMV and PPD indices and local thermal comfort criteria*. Brussels: European committee for standardization.

Content

List of figures

List of tables

List of symbols and acronyms

CLT	Cross-laminated timber
TES	Timber element system
G_d	Permanent load $[N]$
$WInt$	Wind Interactive, calculation tool for wind loads
$v_{b,0}$	Basic wind velocity $[m/s^2]$
W_d	Wind load $[N]$
l_{ef}	Screwing-in depth, anchor length $[mm]$
d	Screw diameter $[mm]$
$F_{ax,k}$	Characteristic withdrawal resistance $[N]$
k_{mod}	Modification factor for load duration and moisture content
γ_m	Material factor
k	Conversion factor per number of screws
$R_{ax,d}$	Design withdrawal resistance $[kN]$
$F_{v,Rk}$	Shear capacity per shear plane per fastener $[N]$
$R_{v,d}$	Design shear capacity $[kN]$
n_{req}	Required number of connections
λ	Thermal conductivity $[W/mK]$
T_i	Internal air temperature $[°C]$
T_e	External air temperature $[°C]$
U	U-value, thermal transmittance $[W/m^2K]$
R	Thermal resistance $[m^2K/W]$
ϕ	Heat flux $[W]$
T_s	Surface temperature $[°C]$
f_{Rsi}	Temperature factor [-]
PMV	Predicted mean vote
PPD	Predicted percentage dissatisfied [%]
PD_v	Percentage dissatisfied for vertical temperature difference [%]
PD_r	Percentage dissatisfied for radiant asymmetry [%]
ΔT	Temperature difference [°C]

1 Introduction

In the recent years, prefabrication of timber façade elements has become a more and more researched topic. However, most of the recent research focusses on using prefab systems for façade renovation. This study will investigate the possibility of prefab façade systems for newly built constructions, in particular with a cross-laminated timber substructure (CLT). CLT is one of the most widely used timber products nowadays and has a lot of beneficial properties.

1.1 Façade prefabrication

In the last decade, there has been a lot of development in the research on prefab façade elements for renovation purposes. One of the most well-known renovation systems is the TES-method [1]. TES is a timber based element system with the goal to improve building's energy efficiency by renovating the building envelope. There are a lot of different timber based element systems, but the principle is always the same. A prefabricated insulation panel is attached on the outside of the existing façade, which is either (partly) demolished or just the way it was before. Most of the buildings that were built from '50 to '80 don't meet the current energy regulations anymore. That's why it's the case in a lot of countries that when an (old) building is being renovated, it must meet the new energy performance regulations. The best way to do this is by retrofitting the external walls [2].

Figure 1 – TES, timber element based systems [1] [3]

But next to prefab systems for renovation, it's also possible to construct new buildings with prefabricated façade elements. They are already applied for a while now, take for example prefab concrete sandwich panels or prefab cladding panels with a steel or aluminium substructure. Prefab systems have a lot of advantages, construction speed is one of the most important benefits.

The construction time on-site decreases, which means that the cost of man hours decreases and that the building can be erected in much less time. However, timber based prefab systems aren't very popular. And yet, they could have a lot of advantages. Timber frame systems are very light, not expensive and easy to handle. The biggest disadvantage is that they are only applicable for low or mid-rise construction. CLT, has higher strength properties, which means that it could be possible to build higher. That's why it is interesting to further look into CLT based façade systems.

1.2 Cross-Laminated Timber

During the last decades, Cross-Laminated Timber (CLT) has become one of the most used engineered wood products for building construction. Recently, Gasparri et al. investigated the possibility of prefabricated CLT based façade elements [4] [5] [6]. To get a better understanding of this construction material, it is important to discuss the most important properties of CLT first.

CLT or cross-laminated timber is an engineered wood product that consists out of several layers of timber board, stacked in perpendicular direction on each other and glued together. There are usually three of five layers. This odd number of laminations means that the outer layers are oriented in the same direction. The direction parallel to grain from the outer layers is considered the major strength direction of the CLT panel, but CLT has load-bearing capacities in both directions. This cross-lamination gives CLT a large load-bearing capacity, which makes it a valid alternative for reinforced concrete. In the case of wall elements, the outer CLT layers are oriented parallel to the gravity loads to maximize the load-bearing capacity. Since CLT is an engineered timber product, it is in fact always prefabricated with pre-cut openings for doors or windows (Figure 3).

Figure 2 – Cross-laminated timber panels [7]

Figure 3 – CLT wall panel with pre-cut openings [7]

CLT has a lot of advantages [8]. The first one is the high construction speed. It just needs to be transported to the construction site and mounted into place. Another advantage is the design flexibility. CLT can be used for floor or roof constructions, but also for walls. It can be combined with other building materials and adjustments can be done on-site with simple tools. Compared

to steel and concrete, CLT has a light weight, but it is of course heavier than a timber frame structure. Although people often associate timber with fire risks, CLT has excellent fire performances. When wood is exposed to fire, the outer layer catch fire but the wood chars very slowly. Then, the char protects the inner part of the wood from further fire propagation (Figure 4). And because of their thickness, the CLT panels can maintain their load-bearing capacity for a long time during fire. Another advantage of CLT is its excellent seismic performance. In Japan, researchers had tested a seven-storey CLT building in an earthquake simulation (Figure 5). Their tests resulted in almost no deformation of the structure [8]. CLT has also very good thermal performances. First, timber has a relatively low thermal conductivity compared to steel or concrete. Second, the CLT panels have a high thermal resistance because of their extra thickness. This means that the façade needs less thermal insulation if necessary. And since CLT can store a significant amount carbon, it is also a very environmental building solution. An important parameter to consider when working with timber products, is the moisture content. Wood expands and contracts a lot more perpendicular to grain than parallel to grain. With cross-laminated timber the layers are oriented in alternating direction, which decreases the expansion/contraction in both panel directions.

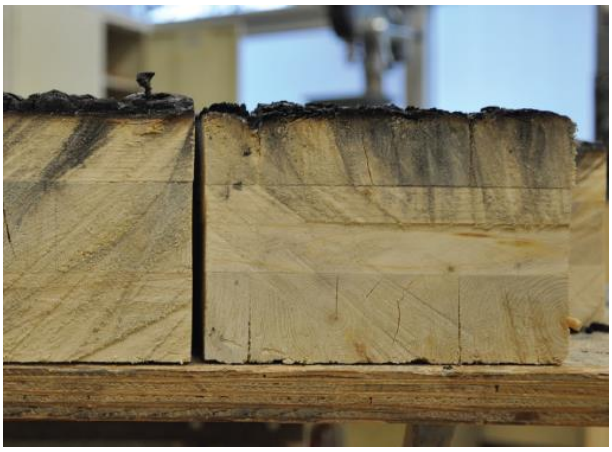

Figure 4 – Charred CLT after fire test [8]

Figure 5 – Japanese earthquake simulation [8]

CLT is not yet included in the Eurocodes, but there is a lot of existing research available. ProHolz, an Austrian magazine for the timber industry, provided a structural design guide with the basic design and engineering principles for cross-laminated timber [9]. CLT can be manufactured in lengths up to 16 m and widths up to 3 m. The thickness of the panels can go up to 300 mm, but the most common thicknesses are 140 mm and 160 mm [10]. One of the biggest manufacturers of CLT in northern Europe is the Finnish company Stora Enso [11]. The most common way to connect

CLT panels to each other is with self-tapping screws. They can be joined along the unloaded longitudinal side of the panel by using a cover strip, a half-lapped joint or by crossed screws (Figure 6). The connection between a CLT wall panel and a CLT floor slab can be carried out with metal brackets.

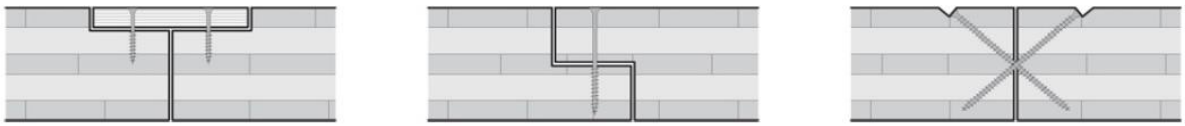

Figure 6 – Joining possibilities along the unloaded longitudinal side, left to right: cover strip, half-lapped joint, crossed screws

Clearly, cross-laminated timber is an interesting material to work with. It has a lot of advantages and could be the perfect solution for prefabricated façade systems.

1.3 Literature survey on CLT façade systems

In the last few years, Gasparri et al. investigated the different possibilities for prefabrication of façade elements for tall CLT buildings. Their research has been presented in three different papers. The first paper investigates the optimal degree of prefabrication and the benefits of prefabrication [4]. The second paper suggests different design setups for a prefab CLT façade system [5]. The last paper investigates the compression perpendicular to grain behaviour of a horizontal joint of the façade system [6], but this will not be further discussed because it isn't part of the scope of this study.

1.3.1 Construction management analysis for tall CLT buildings

In their first paper, Gasparri et al. perform a construction site management analysis for a case study building to investigate the influence of the prefabrication degree on time and costs of the construction project [4]. Prefab envelope systems for timber building have been researched quite frequently in the last years, but most of these researches were focused on timber frame technologies, typical for low or mid-rise construction. Gasparri et al. use a case study building of nine storeys high with a building height of almost 35 m, that has a load-bearing CLT structure. A classic, non-prefabricated, CLT façade has rather unbalanced work phases. The CLT wall panels are mounted on-site, which is very systemized and beneficial for construction speed. But then the rest of the construction phase follows a quite traditional approach where the outer façade layers are completed from the outside through scaffolds. That's why it was interesting to investigate the advantages of increasing the prefabrication degree for tall timber buildings, using CLT as a structural system.

The prefabrication of the façade has a lot of advantages. First, the major part of the manufacturing operations is shifted from the construction site to the production site. This benefits the quality of the construction process. Second, the wooden products are immediately protected from weather agents during the construction phase. Unfavourable weather conditions can affect the quality of the construction. Engineered wood products like CLT require longer times to dry than structural timber. Moisture variation can cause swelling and shrinkage, which is a critical issue for tall timber buildings. The weather can also cause incorrect humidity levels, resulting in mould problems [5]. Some construction projects in the past used large temporary shelter structures to protect the building components, which is not very efficient (Figure 7).

Figure 7 – Temporary protective roofing at a construction site [4]

For their study, Gasparri et al. considered two different construction options. Option A is with non-prefabricated CLT wall elements, following the current work method for CLT structures. CLT panels are transported to the construction site with trucks and mounted in their final positions with cranes. Then the external layers are installed on-site, working from scaffolds. Option B is the entirely prefabricated solution were the workers can operate from the designated floor without the use of scaffolds. The prefab elements contain insulation, finishing layers and windows. This way, there is no work necessary from the outside through scaffolds. The work phases for both options are shown in Table 1.

Table 1 – Work phases for option A and B [4]

	Option A	Option B
a	Excavation for foundations	Excavation for foundations
b	Reinforced concrete foundations construction	Reinforced concrete foundations construction
c	Reinforced concrete load-bearing walls construction	Reinforced concrete load-bearing walls construction
d	Concrete slab construction	Concrete slab construction
e	First and second level of scaffolding installation	–
f	Vertical load-bearing CLT panels installation	Vertical load-bearing CLT panels installation
g	Horizontal CLT panels	Horizontal CLT panels
h	Repetition of e, f, g phases $n-1$ times, where n is the building storey number	Repetition of f, g phases $n-1$ times, where n is the building storey number
i	Thermal insulation installation	–
l	Waterproof canvas installation	–
m	External finishing installation	–
N	Scaffolds dismantling	–

Both options make a distinction between large size panels (A-LP and B-LP) and small size panels (A-SP and B-SP). The large panels are beneficial for the construction speed, but small size panels result in a higher architectural freedom and are easier to transport and handle. The façade build-up for both option A and B is the same. It consists, from interior to exterior, out of: CLT structural panel, breathable vapour barrier, wood fibre insulation layer of 10 cm, breathable waterproofing membrane and a wooden vented façade. A vented façade has the advantages of keeping the wall dry and results in better thermal performances. But it could be interesting to investigate more in depth the different possibilities of the cladding system to give designers architectural freedom in customizing the façade.

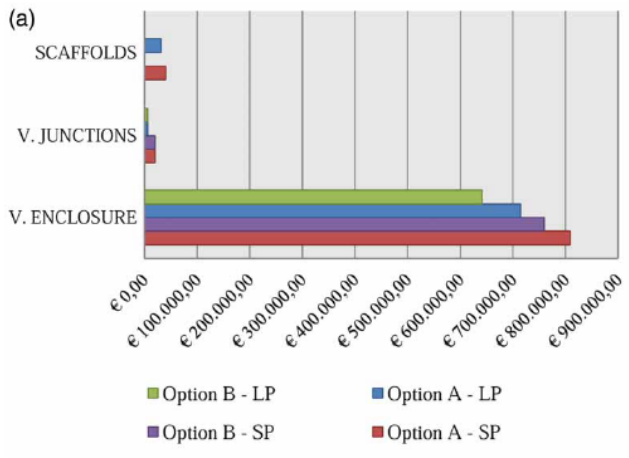

Figure 8 – Partial price graphic comparison for the four design options [4]

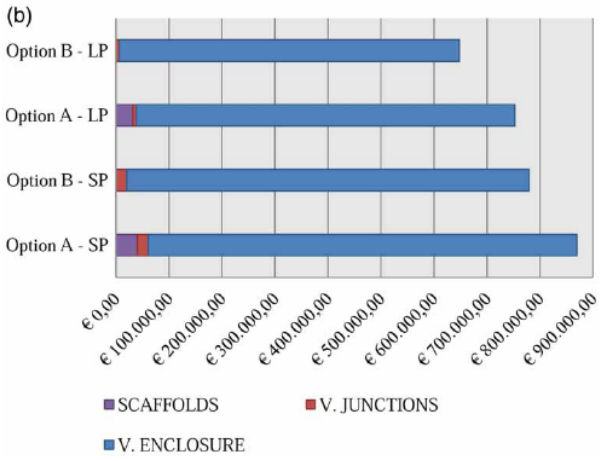

Figure 9 – Total price graphic comparison for the four design options [4]

The cost analysis performed by Gasparri et al. confirms that prefabrication provides a cost reduction. Their results are shown in Figure 8 and Figure 9. Even without considering the costs for the scaffolds, is option B more cost efficient than option A. Table 2 shows the results from the time analysis. Construction with larger panel sizes is a lot faster than with small panel sizes. An explanation for this difference is the extra manpower needed for loading more smaller panels on the trucks and more on-site handling. Also note the difference between the sum of durations and the actual duration for option A. This is because some activities can be performed simultaneously. This isn't the case for the prefabricated design options, but they are still faster than the non-prefabricated ones.

Table 2 – Sum of partial durations and actual duration of the different design options [4]

Days	Option A – SP	Option B – SP	Option A – LP	Option B – LP
Sum of durations	207.00	81.00	162.00	29.25
Actual duration	103.25	81.00	85.75	29.25

Figure 10 compares the results of the cost analysis with the time analysis. The study from this paper proves that off-site prefabrication of façade elements results in a significant reduction of costs, especially if larger panel sizes are used. So, it can be concluded that prefabricated CLT façade systems for tall timber buildings are definitely worth of further research.

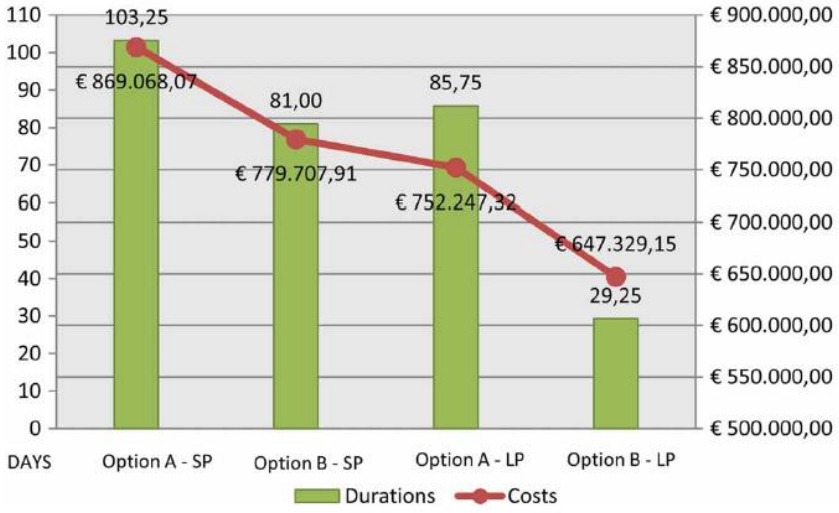

Figure 10 – Construction cost and time comparison for the different design options [4]

1.3.2 Design of prefabricated CLT façade systems

In their second paper, Gasparri et al. present different design setups for a prefabricated CLT façade system [5]. The prefab system has a maximum prefabrication degree, so it includes all external layers of the façade. This way, all the work on-site can be performed from the inside of the building in dry conditions. The external wall element has two functions. The first part is the CLT, which is load-bearing. The second part is the façade, which has the task to protect the CLT and the inside of the building from the weather conditions. To do this, the façade contains two water barriers. The first is called the *water-shedding surface*, this is the cladding of the element. The function of this barrier is to deflect and drain rainwater. In this case, the façade has a ventilated rain screen. This creates a higher flexibility from an architectural point of view. The second water barrier is the *water-resistive barrier*. This is a water-tightness layer that prevents water from penetrating the internal layers. It is important that this barrier is vapour-permeable.

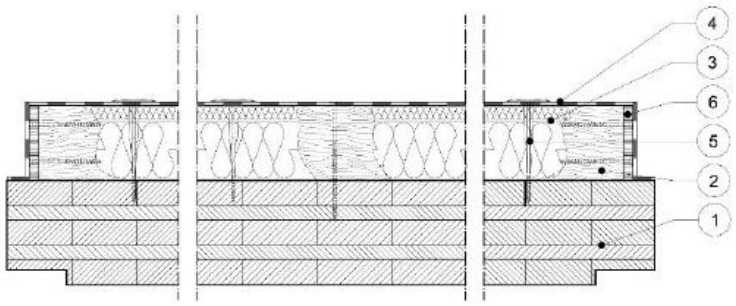

1. Cross-laminated timber, ρ= 470 kg/m³
2. Timber transom, sec. 50 x 100 mm, ρ=510 kg/m³
3. Double density rock wool insulation panel, λ=0,035 W/mK, th. 100 mm, ρ=70 kg/m³
4. Synthetic breathable 3-layer membrane
5. Insulation plug
6. OSB element for panel frame reinforcement, th. 12,5 mm, ρ=620 kg/m³

Figure 11 – Horizontal cross-section of the base panel [5]

Figure 11 show the build-up of a base panel without the cladding. The insulation is 10 cm of rock wool insulation. The choice for rock wool is because of its low weight, which is beneficial for transportation and handling of the panels. It is not possible to use synthetic insulation materials because they are bad in combination with timber products. Although they are very light and have excellent thermal performances, they are not permeable and would trap moisture inside the structure. The choice for external insulation is to keep the wood dry and warm and to minimize the risks for moisture damage. In their research, Gasparri et al. discuss different possibilities for the cladding. It is possible to vary in type of substructure (timber, metallic …), fixing system (exposed, concealed …) and finishing material (wooden, ceramic, cement fibreboard, metallic …). But the base panel always stays the same.

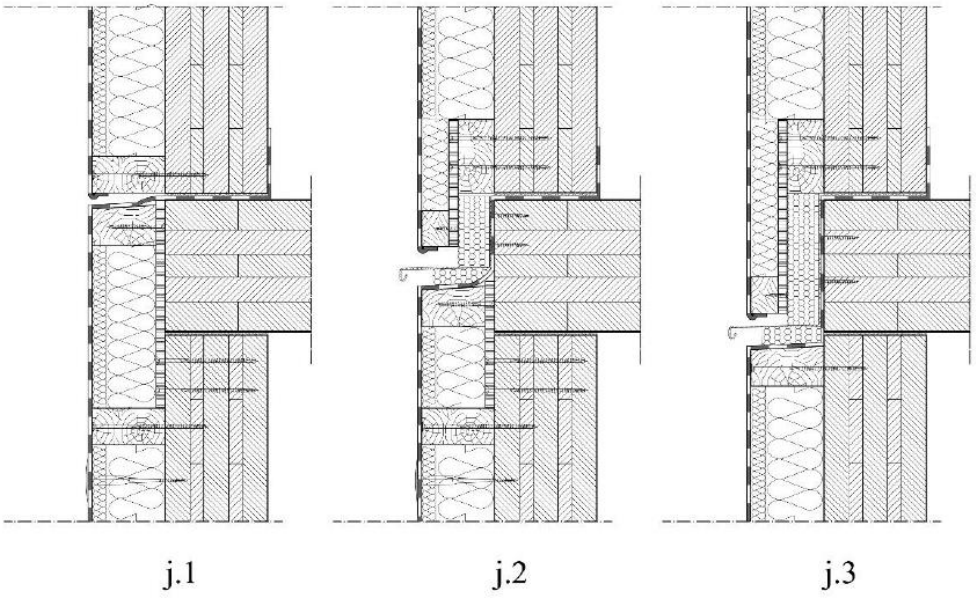

Figure 12 – Horizontal joint positioning options (vertical cross-section) [5]

For the design of the horizontal joint, three options were investigated (see Figure 12). The three design options vary according to the location of the joint relative to the floor level. For the first option (j.1) the façade joint is placed at the upper side of the floor slab. This means that the projecting part of the panel is at the top of the panel. This has advantages for transportation, the panels can just stand during transport. The big disadvantage of this joint setup is the air and water tightness, which is much better handled in the other two options. Setup j.2, which is placed at the middle of the floor slab, is more reliable for this matter. The disadvantage for this joint type is that now both sides of the panel have projecting parts, which makes it impossible to transport them standing and makes them a more vulnerable system. The third setup, j.3, has the joint located at the bottom part of the floor slab. This makes this joint type the best solution regarding air and water tightness, but still vulnerable during transport. According to Gasparri et al. is joint type j.3 the best solution, because it's the most reliable joint solution.

A cross-section of the horizontal joint with cladding is shown in Figure 14, a 3D visualisation is shown in Figure 15. In this example, the cladding consists of vertically oriented fir wood planks fixed through screws on two wood mullions (one horizontal, one vertical). The projected part of the façade panel is reinforced with an OSB element. The joint itself is filled with low density rock wool insulation. There are also small compressible insulation mats between the face of the CLT wall panels and the CLT slab that prevents air flow.

The vertical joint is shown in Figure 13. The vertical joint is realized by installing a wooden strip from the inside of the building to connect two wall panels with each other. In this case again, low density insulation has been used in the joint to interrupt the thermal bridging.

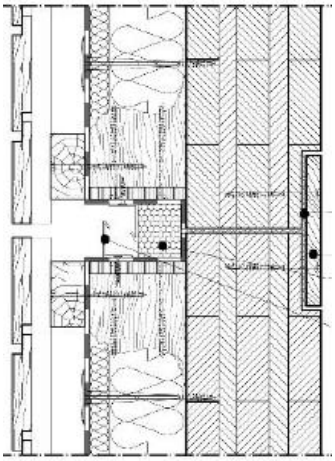

Figure 13 – Vertical joint (horizontal cross-section) [5]

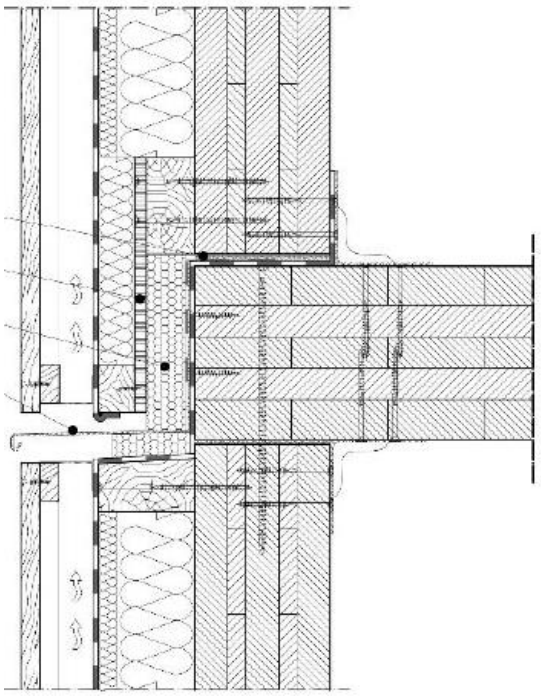

Figure 14 – Horizontal joint (vertical cross-section) [5]

The installation of the prefab panels follows a systematic work flow. First, the load-bearing wall system is erected at a certain floor. Next, the upper floor is installed, supported by the load-bearing wall. Then, the horizontal joint is completed from the just installed floor and all water-tight membranes are positioned. The metal flashing/fire barrier is installed along the perimeter and the soft insulation mat is placed. Then, the first upper wall elements are mounted and the vertical joints between them are completed. Once all wall panels are erected on that floor, the next floor can be installed and the process can be repeated.

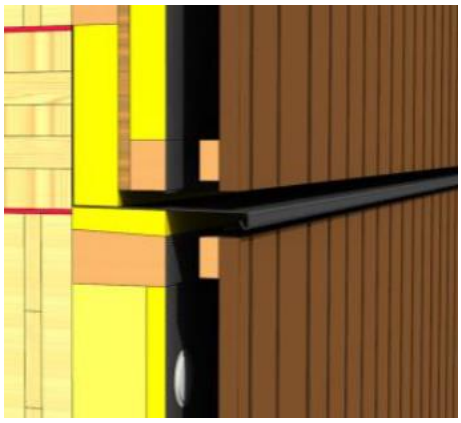

Figure 15 – 3D visualisation of the horizontal joint [5]

2 Aim and scope

2.1 Scope

According to the literature study just mentioned, it is clear that prefabricated CLT-façade systems have a lot of potential [4] [5]. It is also clear that a lot of old buildings don't meet the current energy efficiency regulations and that their façade must be renovated [2]. Since it's difficult to predict the energy requirements in the future, it could be interesting to look into façade systems that are easily replaceable. This way, the façade insulation could be easily replaced or increased to meet the new requirements. But even if the façade doesn't have any problems regarding the energy requirements, it could still be beneficial to renew the cladding. For instance, if the maintenance of the façade has been neglected and the cladding shows ugly spots. Or even if the cladding isn't damaged but simply outdated regarding the style. Think about the added value to a building if it has a façade that can be easily replaced.

The challenge of a system of this kind is the way the façade elements are connected to the load-bearing substructure, in this case a CLT wall. The first solution that comes to mind, is to attach the cladding with a small amount of connections that are directly anchored into the CLT. This raises the question of the effect on heat transfer through these bigger connections. First of all, the insulation will be completely penetrated, which creates a thermal bridge. Secondly, if the number of connections is limited, the diameter will be larger, which increases the effect of the thermal bridge.

2.2 Aim and research method

In this study, the effect of large-diameter-connections on heat transfer and thermal bridging will be investigated. In order to investigate the consequences of these connections, several models will be simulated with Comsol Multiphysics. Therefore, a simplified model of the façade system will be designed. To design these models, it is important to have an idea about the loads acting on the façade to determine the required number of connections. After these models have been simulated with Comsol, the results will be analysed and discussed. The defining parameters to analyse will be the U-value of the façade and the internal surface temperature. Based on these parameters a conclusion on the effect of large-diameter connections will be formulated.

3 Research

3.1 Connection design

The main concept of this study is to investigate the effects on heat transfer if the cladding elements are attached with a smaller amount of larger connections. It is therefore important to determine the required number of connections in function of the diameter. But to do this, the loads acting on the connection must be calculated first.

3.1.1 Permanent load

The defining loads will be the self-weight of the cladding element and the wind suction on the façade. The permanent loads of the cladding element are calculated by multiplying the density ρ of each member i with its volume V and with the gravitational acceleration g (9,81 m/s^2):

$$G_{k,i} = \rho_i . V_i . g \; [N] \tag{1}$$

Then the permanent loads are added together and multiplied with a partial factor of 1,35:

$$G_d = 1{,}35 . \Sigma G_{k,i} \; [N] \tag{2}$$

It's important to note that this study assumed that the façade elements didn't contain any windows. Glass elements could have a big influence on the self-weight of the façade element.

3.1.2 Wind load

The wind suction has been determined by making use of the calculation tool *Wind Interactive (WInt)* of the Belgian Building Research Institute, also known as the WTCB [12]. WInt is an application used for a fast and simple calculation of the wind loads on a façade or roof of a simple rectangular building. The calculations are based on EN 1991-1-4 [13]. The wind suction acting on the façade depends on several parameters, it goes without saying that the wind loads are different for each specific case. For this study, the wind loads are calculated for a building with a height of 15 m and a ground area of 30 x 12 m^2. The basic wind velocity $v_{b,0}$ is mentioned in the national annexes and is depending on the geography. For Finland $v_{b,0}$ varies from 21 m/s in the mainland to 22 m/s in sea areas [14]. For Belgium $v_{b,0}$ varies from 23 m/s to 26 m/s [15]. In this case, the wind load has been calculated with a basic wind velocity of 23 m/s. The terrain category describes the surrounding environment of the building site. In this case a terrain category II has been used. This means that the surrounding area has low vegetation such as grass and isolated obstacles (e.g. trees, buildings) with separations of at least 20 times the height of these obstacles. The wind

direction has been chosen in a way that there is suction on the main façade. Figure 16 shows the input that is used for the calculation.

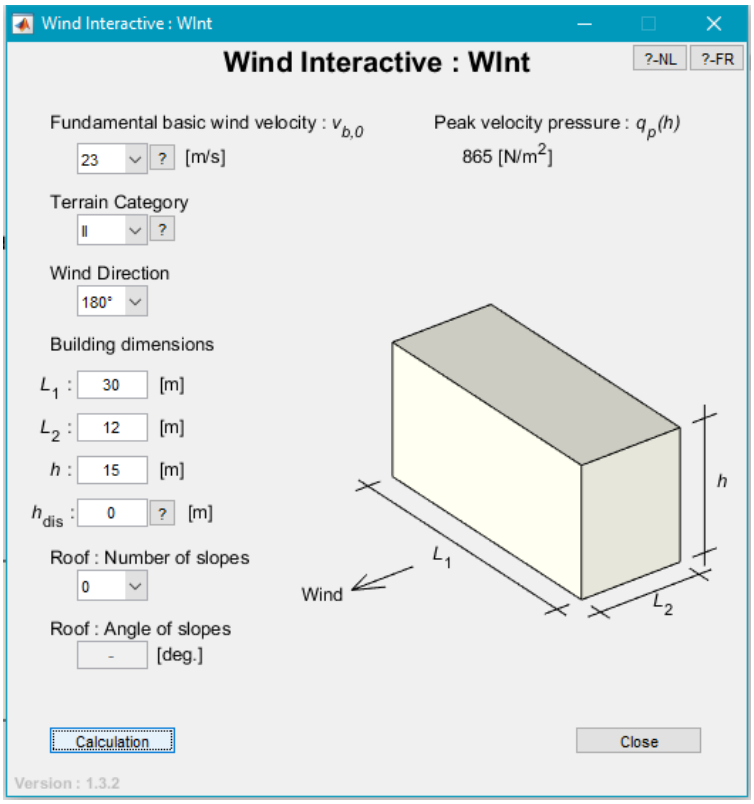

Figure 16 – WInt input

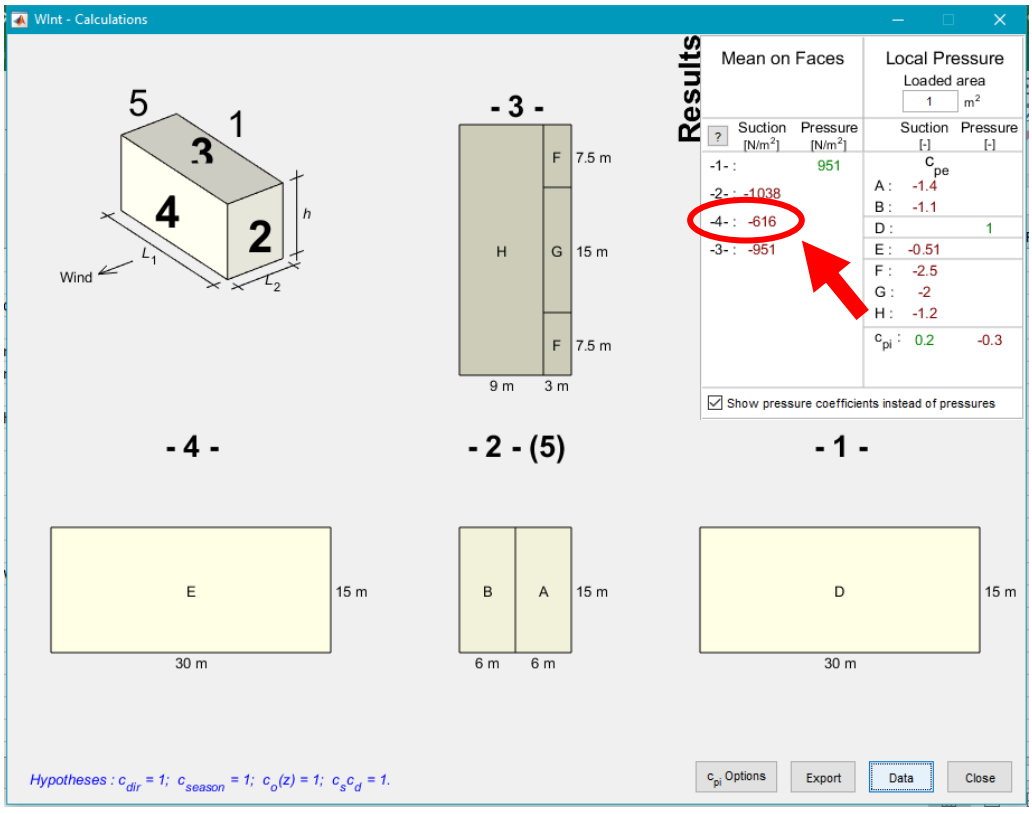

Figure 17 – WInt output

The results for the wind calculation are shown in Figure 17. The mean wind suction w_k on the façade has a value of 616 N/m^2. Now, to determine the wind load acting on the connection, this value must be multiplied with the area of the cladding element and with a partial factor of 1,5:

$$W_d = 1{,}5 . w_k . A \; [N] \tag{3}$$

Now that the loads are known, the capacity of the connections can be calculated. The permanent loads will act as a lateral shear force on the connection (Figure 19), while the wind suction will act as an axial withdrawal force (Figure 18). The general calculation principles for the load-bearing capacity of connections are stated in EN 1995-1-1 [16]. However, cross-laminated timber is not yet included in Eurocode 5. Therefore, the calculations for the load-bearing capacity are based on the CLT design guide of proHolz [9]. This design guide also refers to the Eurocode with sometimes some minor changes to the equations.

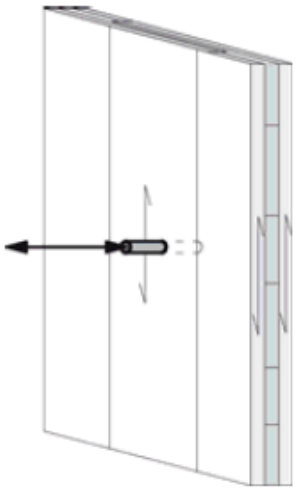

Figure 18 – Fastener subjected to withdrawal

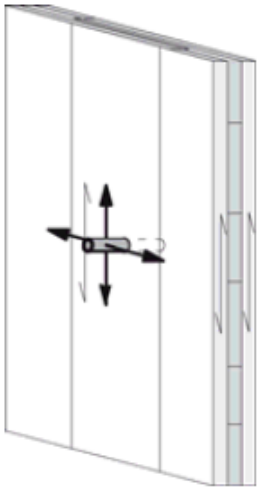

Figure 19 – Fastener subjected to shear

3.1.3 Withdrawal resistance

Self-tapping screw subjected to withdrawal forces must have a minimum diameter of 6 mm and must have a screwing-in depth l_{ef} of at least three board layers and $l_{ef} \geq 8.d$. There must also be at least two screws per connection or per row of fasteners. The board layer build-up for CLT140 is 40 mm for the outer layers and three layers of 20 mm in between. For CLT160 the middle layer is also 40 mm [10]. This means that for CLT140:

$$l_{ef,CLT140} = \max(80; 8.d) \tag{4}$$

and for CLT160:

$$l_{ef,CLT160} = \max(100; 8.d) \tag{5}$$

According to the design guide of proHolz, the characteristic withdrawal resistance $F_{ax,k}$ is:

$$F_{ax,k} = \frac{31.d^{0,8}.l_{ef}^{0,9}}{sin^2(\epsilon) + 1{,}5.cos^2(\epsilon)}\ [N] \tag{6}$$

Where:

d	is the outer thread diameter of the screw;
l_{ef}	is the penetration depth of the screw in the CLT;
ϵ	is the screw-in angle to the fibre.

Since the screw-in angle to the fibre is 90°, equation (6) can be simplified to:

$$F_{ax,k} = 31.d^{0,8}.l_{ef}^{0,9}\ [N] \tag{7}$$

This characteristic value must then be multiplied with a k_{mod}-factor and divided by a material factor γ_m. As mentioned before, CLT is not yet included in the Eurocode, this means that there is no standard value for γ_m yet. For the rest of the study, $\gamma_m = 1{,}25$ and $k_{mod} = 0{,}8$ will be considered. Since these equations from the proHolz design guide are drafted for connections with four screws, it is also necessary to multiply $F_{ax,k}$ with a conversion factor per number of screws k. The values of k are given in Table 3.

Table 3 – Conversion factor per number of screws

Number of screws	2	4	8	12	16
k	1,07	1,00	0,93	0,90	0,87

This makes that the design withdrawal resistance of the connection is:

$$R_{ax,d} = \frac{k_{mod}}{\gamma_m}.k.F_{ax,k}.10^{-3}\ [kN] \tag{8}$$

3.1.4 Shearing-off resistance

Self-tapping screws exposed to shear must have a minimum diameter of 6 mm and the screw-in depth must be at least three CLT board layers. The capacity per shear plane of each fastener $F_{v,Rk}$ is determined according to the European Yield Model, stated in EN 1995-1-1. The connection will only have one shear plane, namely between the mullions and the CLT. This means that $F_{v,Rk}$ is the lowest value of the six expressions from equation (9):

$$F_{v,Rk} = \min \begin{cases} f_{h,1,k} t_1 d & \text{(a)} \\ f_{h,2,k} t_2 d & \text{(b)} \\ \frac{f_{h,1,k} t_1 d}{1+\beta} \left[\sqrt{\beta + 2\beta^2 \left[1 + \frac{t_2}{t_1} + \left(\frac{t_2}{t_1} \right)^2 \right] + \beta^3 \left(\frac{t_2}{t_1} \right)^2} - \beta \left(1 + \frac{t_2}{t_1} \right) \right] + \frac{F_{ax,Rk}}{4} & \text{(c)} \\ 1{,}05 \frac{f_{h,1,k} t_1 d}{2+\beta} \left[\sqrt{2\beta(1+\beta) + \frac{4\beta(2+\beta) M_{y,Rk}}{f_{h,1,k} d \quad t_1^2}} - \beta \right] + \frac{F_{ax,Rk}}{4} & \text{(d)} \\ 1{,}05 \frac{f_{h,1,k} t_2 d}{1+2\beta} \left[\sqrt{2\beta^2(1+\beta) + \frac{4\beta(1+2\beta) M_{y,Rk}}{f_{h,1,k} d \quad t_2^2}} - \beta \right] + \frac{F_{ax,Rk}}{4} & \text{(e)} \\ 1{,}15 \sqrt{\frac{2\beta}{1+\beta}} \sqrt{2 M_{y,Rk} f_{h,1,k} d} + \frac{F_{ax,Rk}}{4} & \text{(f)} \end{cases} \quad (9)$$

These six expressions correspond to the six possible failure modes of Figure 20. Failure mode (a) and (b) describe the embedment failure of the timber/CLT. Failure modes (c) to (f) describe the yield failure of the fastener. On Figure 20, the left member (member 1) corresponds to the mullions, while the right member (member 2) corresponds to the CLT. Please note that in this case the screw doesn't penetrate the CLT completely, but the principle is the same.

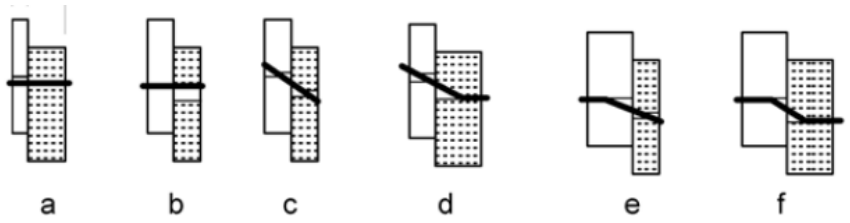

Figure 20 – Different failure modes of the European Yield Model

Looking more detailed into equation (9) where:

t_1	is the thickness of the mullions;
t_2	is the penetration depth of the screw in the CLT;
d	is the outer thread diameter of the screw;
$f_{h,i,k}$	is the characteristic embedment strength of the member;
β	$= \frac{f_{h,2,k}}{f_{h,1,k}}$;
$M_{y,Rk}$	is the characteristic fastener yield moment;
$F_{ax,Rk}$	is the characteristic axial withdrawal capacity of the fasteners, as in equation (6).

The embedment strength $f_{h,k}$ for fully threaded self-tapping screws is according to the design guide:

$$f_{h,k} = 0{,}019.\rho_k^{1,24}.d^{-0,3}\ [N/mm^2] \tag{10}$$

Where ρ_k is the characteristic bulk density of the material, for CLT this is 400 kg/m^3.

The fastener yield moment is calculated as:

$$M_{y,Rk} = 0{,}3.f_{u,k}.d^{2,6}\ [N.mm] \tag{11}$$

Here is $f_{u,k}$ the tensile strength of the fastener, for self-tapping screws is $f_{u,k} = 800\ N/mm^2$.

Here again, the characteristic value $F_{v,Rk}$ must be multiplied with the same k_{mod} and γ_m-values to obtain the design value:

$$R_{v,d} = \frac{k_{mod}}{\gamma_m}.F_{v,Rk}.10^{-3}[kN] \tag{12}$$

3.1.5 Required number of connections

Now to determine the required number of connections n_{req}, the loads must be divided by the capacity of the connection. This means that the permanent loads G_d must be divided by the shear capacity $F_{v,d}$ and that the wind suction W_d must be divided by the withdrawal capacity $F_{ax,d}$. This makes the following equation:

$$n_{req} = \max\left(\frac{G_d}{R_{v,d}}; \frac{W_d}{R_{ax,d}}\right) \tag{13}$$

The calculations show that in all cases the ratio $W_d/R_{ax,d}$ was governing because of the low value of G_d.

Looking at all the different equations, the only variable parameters for n_{req} are the area of the cladding element, the screw diameter and the penetration depth in the CLT, which depends on the CLT thickness. Figure 21 and Figure 22 show the correlation between all these factors. The figures plot the required number of screws in function of the element surface area for each screw diameter. The left graph does this for CLT of 140 mm, the right one for CLT of 160 mm. Since the minimum thickness of the CLT element is 10 times the screw diameter [9], screws with a diameter of 16 mm are only possible with CLT160. It is important to remember that according to the requirement for withdrawal resistance, there must be at least two screws per connection or per row of fasteners and that the amount of screws varies by steps of 4. So essentially the number of screws is either 2, 4, 8, 12 or 16 (see also Table 3). This means that n_{req} should always be round up to one of these values. Every time one of these values is crossed (e.g. $n_{req} = 4$), a jump in the graph is visible. This corresponds to the correction factor from Table 3.

From the graphs can be concluded that there aren't many screws necessary as long as the dimensions of the cladding elements aren't too large. For example, a CLT140-panel of 3 x 4 m^2 with screws of 8 mm requires only 2 screws ($n_{req} = 1{,}92$), while a CLT160-panel of 3 x 10 m^2 with screws of 16 mm also has enough with 2 screws ($n_{req} = 1{,}60$).

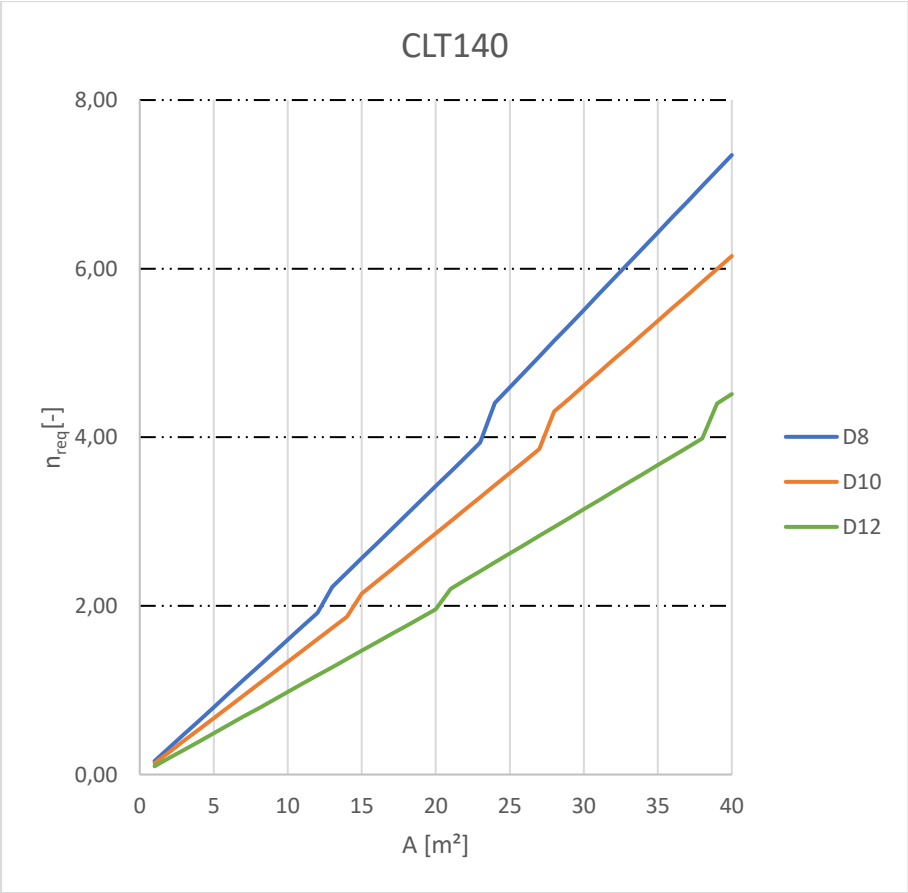

Figure 21 – Required number of screws for CLT140

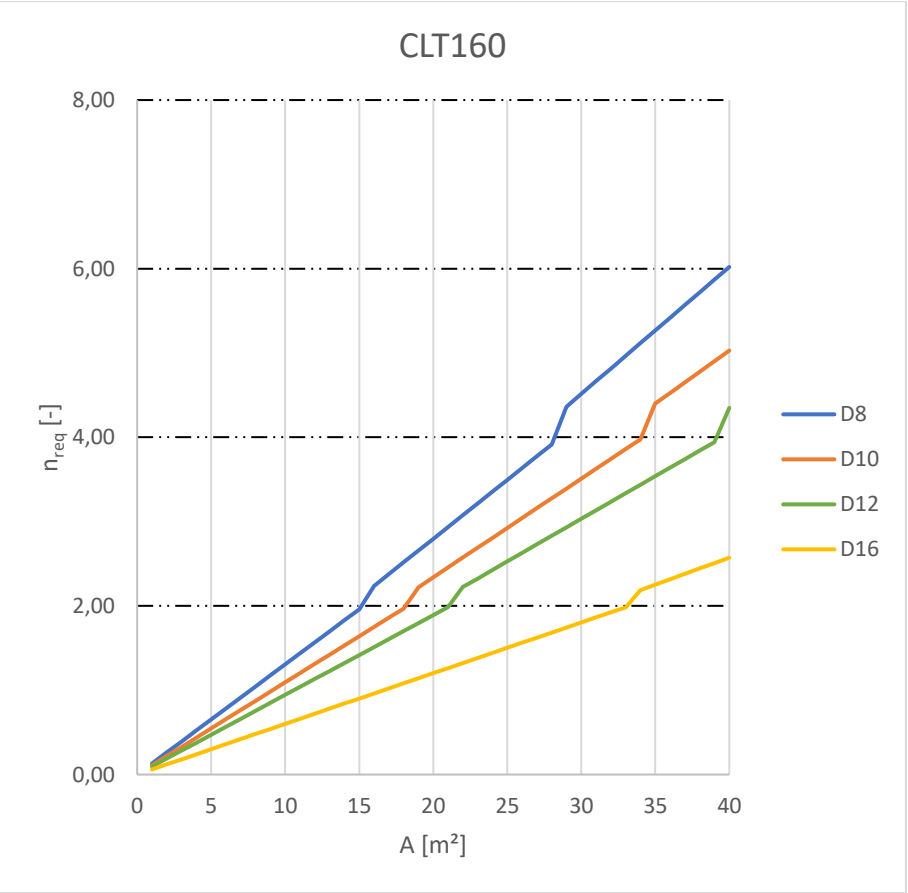

Figure 22 – Required number of screws for CLT160

3.2 Model design

As said before, the focus of this study is more on the consequences of large-diameter-connections than on the design of the façade system. Therefore, the design will be based on the research of Gasparri et al. [4; 5]. Their research discusses two different work methods, one completely built on-site, the other one completely prefabricated. In their prefabricated system, the cladding, insulation and CLT form one façade element. In this study however, the load-bearing CLT-panel will be separated from the prefabricated cladding element. It may be possible to place both CLT and cladding as one element on-site and then replace only the cladding element in a later stage, but this was not investigated in this study. So, for the rest of this research, we assume that the CLT element is mounted on-site separately from the cladding element.

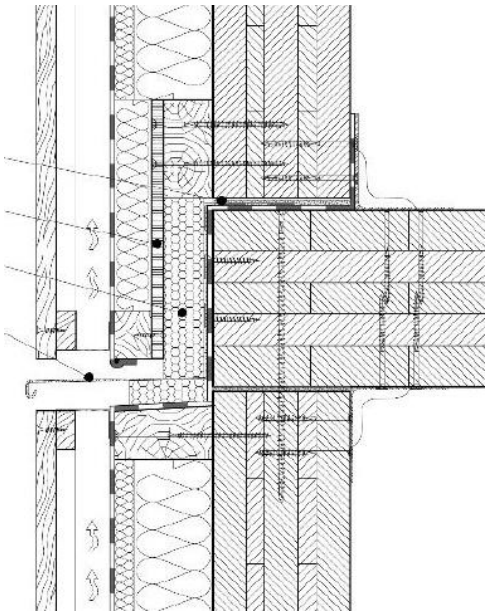

Figure 23 – Joint detail of the model of Gasparri et al. [5]

The build-up of the simulated model is based on the one of Gasparri. From the inside to the exterior there is a load-bearing CLT panel, a timber frame with rock wool insulation, two timber mullions and finally a wooden cladding. The cladding in this model are vertically oriented wood planks and are fixed to the timber mullions. This way, a ventilated cavity is created. According to EN ISO 6946:2007 [17], the thermal resistance of well-ventilated air layers and all other layers between the cavity and the external environment can be disregarded. This means that it's in essence not necessary to model the cladding in the simulation. To verify this, only one model has been made with the cladding (Figure 24), while all other models only have the mullions drawn (Figure 25). According to the code mentioned above, the mullions could also be neglected, but since the connection is made through the mullions there has been decided to keep the mullions present in all models.

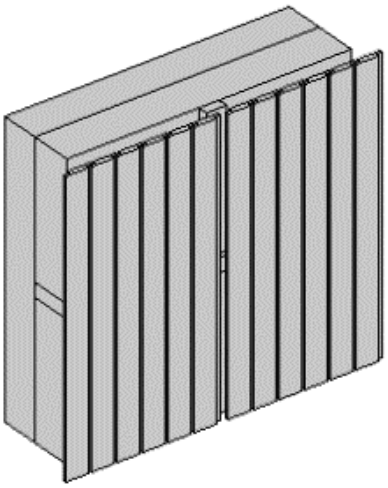

Figure 24 – Simplified Comsol model with cladding

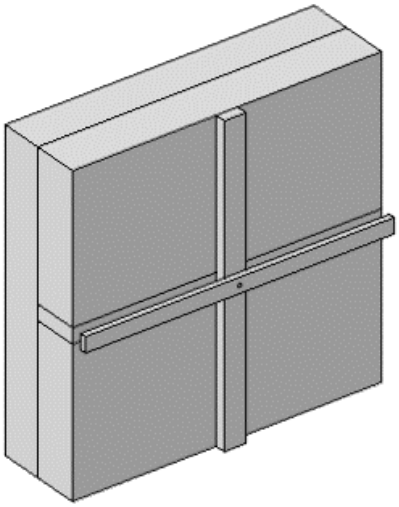

Figure 25 – Simplified Comsol model without cladding

There's been made a distinction in three different types of models, Table 4 gives an overview of all the different models. The first type is a simplified model of 1 x 1 m^2 with the connection through the timber frame and mullions in the centre. This model type varies for the CLT thickness (CLT140, CLT160) and for the screw diameter (D8, D10, D12, D16). There also are two basic models without connections to have a reference.

The second type is also a simplified model but with larger dimensions, it's a panel of 3 x 4 m^2 with two connections to the sides at half height of the panel (Figure 26). This model type also varies for CLT thickness and for the screw diameter.

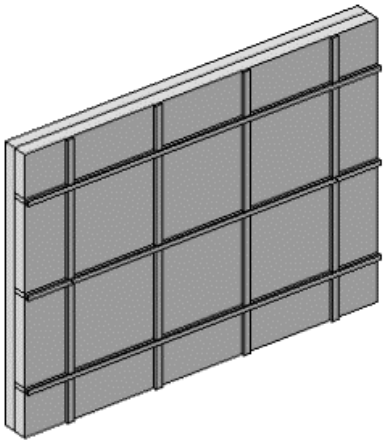

Figure 26 – Large panel model

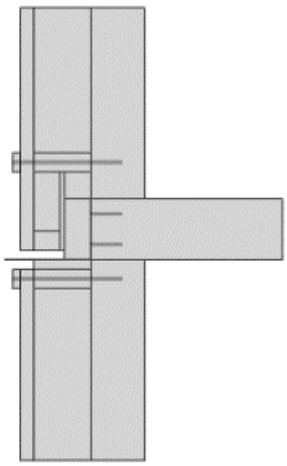

Figure 27 – Floor/wall joint model

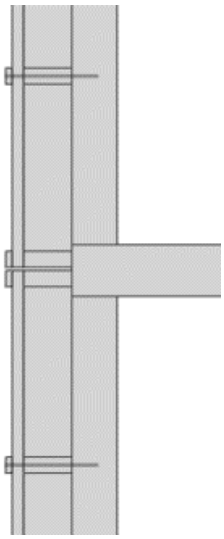

Figure 28 – Different build-up

The third type is a more accurate model of a floor/wall joint with a steel fire barrier (1 mm thick) between the upper and lower floor and with the connections closer to the edge of the elements (Figure 27). All models of this type have a floor slab of CLT160 and an upper and lower CLT panel

of CLT140, the screw diameter is 8 mm. This model type varies for the steel barrier (against the CLT slab, insulation between the barrier and the slab, no barrier) and for the position of the connections (close to the slab, 0.5 m distance from the slab, 1.0 m distance from the slab). Then there is also a model to just look at the floor/wall joint without any connections. Lastly, there is also a completely different build-up of the floor wall joint without any joint insulation (Figure 28).

Table 4 – Overview of the different model types

General model type	*Model specification*	*Code*
1 x 1 m^2	CLT140 w/ Cladding	CLT140-CL
	CLT140 Basic (no connection)	CLT140-B
	CLT140 Diameter 8	CLT140-D8
	CLT140 Diameter 10	CLT140-D10
	CLT140 Diameter 12	CLT140-D12
	CLT160 Basic (no connection)	CLT160-B
	CLT160 Diameter 8	CLT160-D8
	CLT160 Diameter 10	CLT160-D10
	CLT160 Diameter 12	CLT160-D12
	CLT160 Diameter 16	CLT160-D16
3 x 4 m^2	CLT140 Diameter 8	CLT140-3x4-2D8
	CLT140 Diameter 10	CLT140-3x4-2D10
	CLT140 Diameter 12	CLT140-3x4-2D12
	CLT160 Diameter 8	CLT160-3x4-2D8
	CLT160 Diameter 10	CLT160-3x4-2D10
	CLT160 Diameter 12	CLT160-3x4-2D12
	CLT160 Diameter 16	CLT160-3x4-2D16
Floor/Wall joint	Steel barrier against CLT	F/W-barrier_CLT
	Steel barrier w/ insulation	F/W-barrier_ins
	No steel barrier	F/W-no_barrier
	Connection offset 0,5 m	F/W-conn_0.5
	Connection offset 1,0 m	F/W-conn_1.0
	No connections	F/W-no_conn
	Different build-up	F/W-diff

All models are drawn in 3D and use the same materials. The used insulation is double density rock wool with a λ-value of 0,035 W/mK and thickness of 150 mm. All the models have been simulated with an internal air temperature $T_i = +20°C$ and an external air temperature $T_e = -20°C$.

3.3 Simulation

3.3.1 Comsol

All the models have been drawn and simulated in Comsol Multiphysics. Comsol is a physics-based modelling and simulation platform that works on different physics-modules. The module that was used for this research studied the heat transfer in solids by conduction, convection and radiation in a stationary study that is time independent. The models from this study have been simulated and modelled according to the test cases provided in EN ISO 10211:2007 [18], which describes the correct way to calculate heat flows and surface temperatures of 3D thermal bridges. The Comsol website provides model guides of four test cases from the standard. The first two cases are 2D thermal bridges, test case 3 and 4 are 3D thermal bridges. Test case 3 presents a floor/wall-joint and studies the heat conduction of the structure [19]. Test case 4 presents an iron bar through an insulation layer and studies the heat transfer through the iron bar [20]. The results obtained from both models are conform the test cases of the standard. All models that are studied in this research are modelled and simulated according to these two test cases.

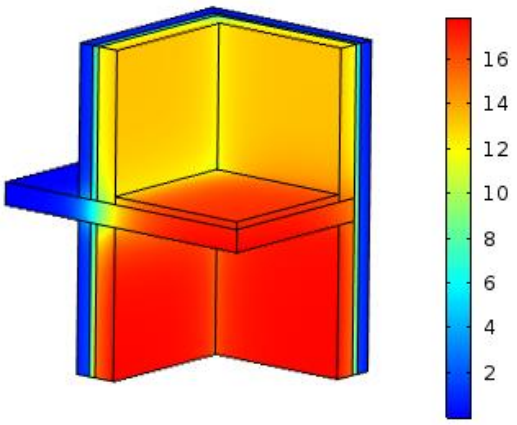

Figure 29 – Temperature distribution of test case 3

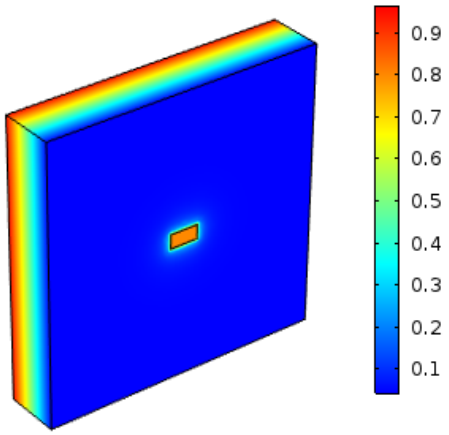

Figure 30 – Temperature distribution of test case 4

3.3.2 Comsol modelling process

By modelling the geometry, Comsol has the possibility to make use of different parameters. This way, when the geometry of the model is drawn with the use of the parameters, the model can easily be changed afterwards by just changing a single parameter. The most important parameters are the thickness of the CLT, the diameter of the screw and the anchor length of the screw.

Each domain of the geometry is assigned a material. Each material has a thermal conductivity λ, a density ρ and a heat capacity at constant pressure C_p. Table 5 gives an overview of the different

materials and their properties. The material properties were either retrieved from the research of Gasparri et al. [5] or from the Comsol material library. The materials OSB and Joint Insulation are only used in the model types of the floor/wall joint.

Table 5 – Material properties

	$\lambda \left[\frac{W}{mK}\right]$	$\rho \left[\frac{kg}{m^3}\right]$	$C_p \left[\frac{J}{kgK}\right]$
CLT	0,11	470	1600
Insulation	0,035	70	1030
Timber	0,13	510	1530
Steel	50	7800	460
OSB	0,13	620	1550
Joint Insulation	0,035	50	1030

To simulate the heat transfer, boundary conditions need to be defined. There are two boundaries, the internal boundary contains the surface of the CLT panel and has an internal air temperature of $T_i = +20°C$. The external boundary definition consists of the boundary surface of the insulation (warm side of the cavity). The timber mullions and the external boundary surface of the connection are also part of the external boundary definition (Figure 32). The external boundary condition is an external air temperature of $T_e = -20°C$. It is important to note that the results will be completely different if the façade doesn't have a well-ventilated cavity. Then the external boundary definition would only contain the boundary surface of the cladding (see also 3.2).

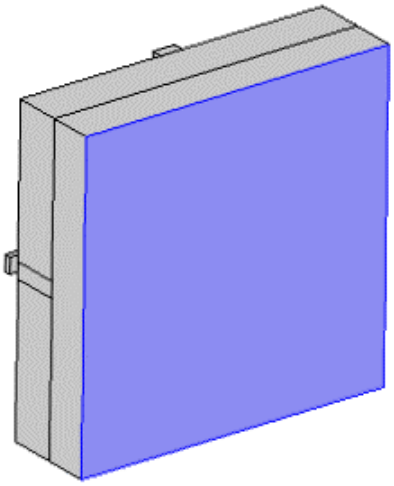

Figure 31 – Internal boundary definition

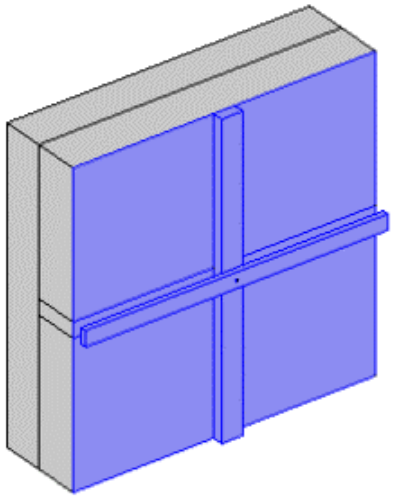

Figure 32 – External boundary definition

Also note that to retrieve more accurate results near the screws, a finer mesh has been used near the steel connections.

3.4 Results

Once the model has been computed and the simulation is complete, the wanted results need to be extracted from Comsol. There are three aspects that need to be obtained from the simulation. The first is a visualisation of the heat flow through the façade, in particular through the connection, in either 2D or 3D. The second requirement is the U-value of the façade or a way to calculate the U-value of the façade. Lastly, the internal surface temperatures are needed to investigate the temperature differences near the connection.

3.4.1 Visualisation of the Heat Flow

Figure 33 shows a 3D temperature plot of the CLT140-D8 model and gives a general image of the temperature distribution. The temperature colour range goes from -20°C to +20°C. However, this plot type gives a nice general image of the temperature distribution, it is difficult to compare multiple model types on this basis.

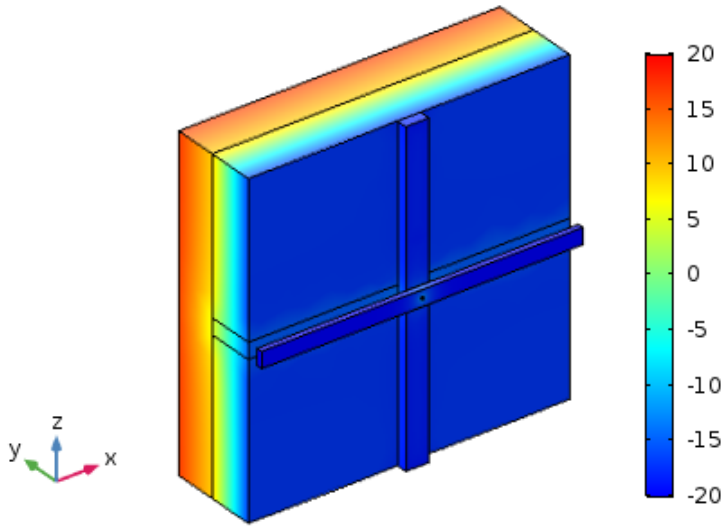

Figure 33 – 3D temperature distribution (CLT140-D8)

Figure 34 shows the temperature distribution in a YZ-plane, cut through the connection. Figure 36 does the same, but for a XY-plane. Both plots show the influence of the steel screw on the heat flow. It is clearly visible that the temperature distribution *deflects* in the neighbourhood of the connection. This is because of the high thermal conductivity of the steel screw. But here again, it is difficult to compare these results for different models.

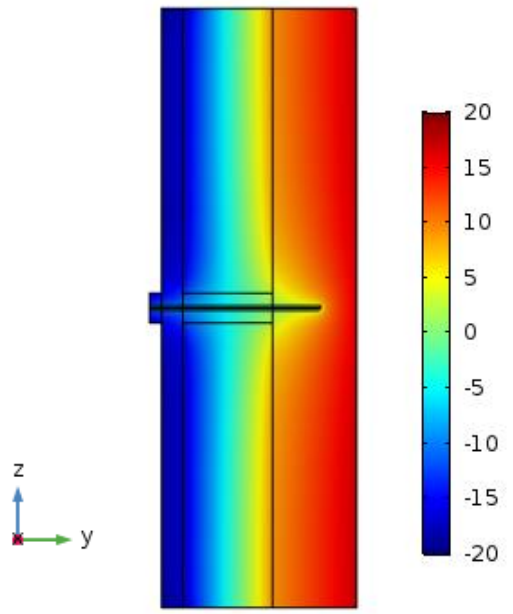

Figure 34 – YZ temperature distribution through the connection (CLT140-D8)

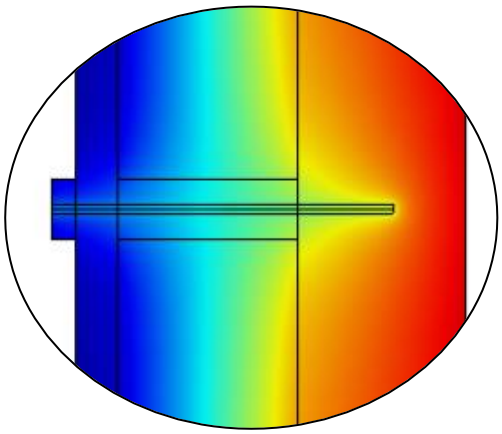

Figure 35 – Close-up of Figure 34

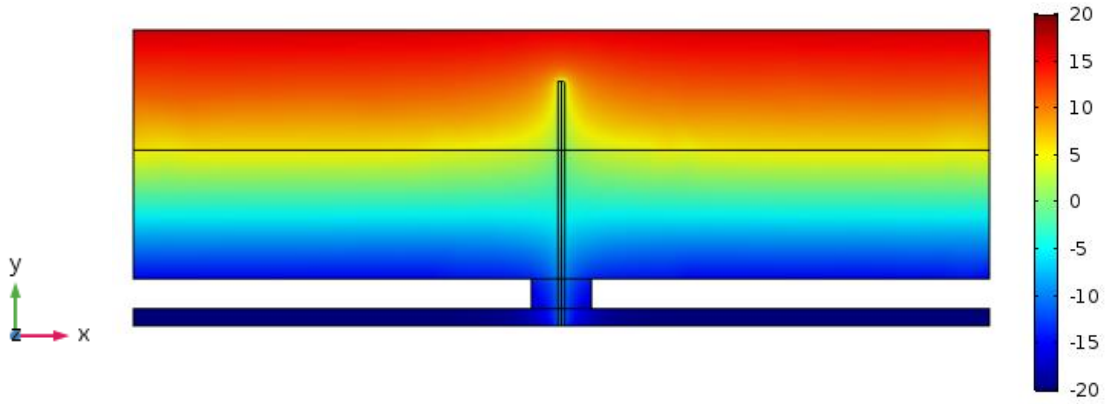

Figure 36 – XY temperature distribution through the connection (CLT140-D8)

Another method to visualize the heat flow is by plotting a temperature curve in function of the y-coordinate. In Comsol, this can be done by creating one cut line in y-direction through the connection and one cut line on the edge of the element. Then, the temperature values on these cut lines can be plotted in function of their position. Figure 37 shows such a temperature curve. The temperature ranges from -20°C to +20°C. A negative y-coordinate indicates that the value is situated on the external side of the façade, thus in the cavity. Since the green curve matches the cut line on the edge, it doesn't cut the mullions and therefore starts from $y = 0\ mm$. The blue line shows the variation of temperature through the steel connection. It is clear that once the end of the connection is reached, the temperature rapidly rises. This is because of the relative good thermal insulation of the CLT.

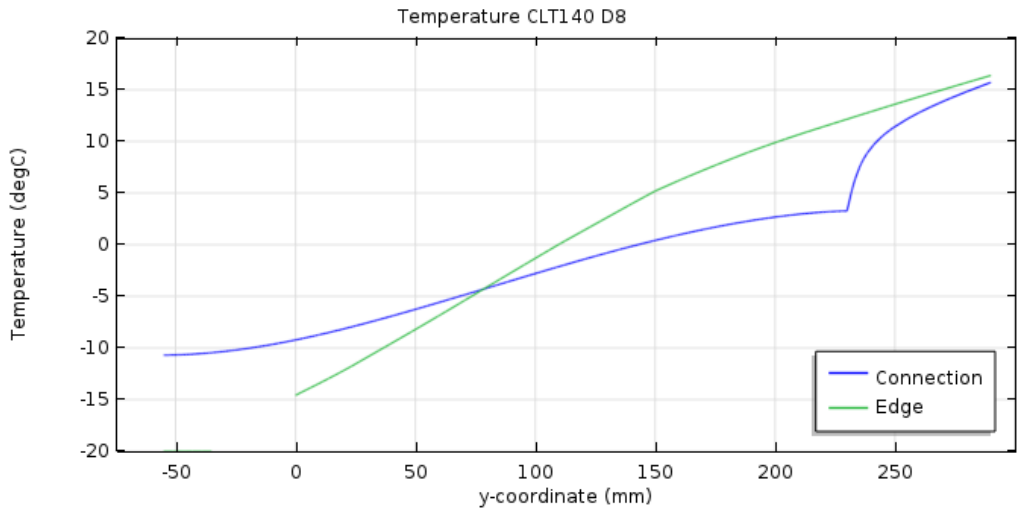

Figure 37 – Temperature curve for CLT140-D8

The advantage of this last plot type is that it's now easier to compare different models with each other. All temperature curves can be found in Annex A. Note that these temperature curves were only created to give a visualisation of the heat flow through the steel connection and are therefore only plotted for the simplified 1 x 1 m^2 models. The other model types would simply show very similar results.

Figure 37 and Figure 38 show the temperature curves for CLT140-D8 and CLT140-D10, respectively. The variable parameter here is the screw diameter. The curves are somewhat different, look for example at the minimum temperature. For CLT140-D8 it lies below -10°C, for CLT140-D10 the minimum temperature is above -10°C. But the difference between the two is not spectacular. Figure 39 shows the temperature curve for CLT160-D8. The variable parameter compared to CLT140-D8 is the thickness of the CLT panel. This has also an effect on the penetration depth of the screw. The anchor length for CLT140-D8 is 80 mm and for CLT160-D8 it is 100 mm (see 0). However, the remaining CLT thickness between the end of the connection and the internal surface is in both cases still 60 mm. But it appears that the extra thickness of CLT does have a certain influence, since the maximum temperature for CLT160-D8 is (slightly) higher than the one for CLT140-D8. But then again, the difference is very small. Figure 40 however, which shows the temperature curve for CLT160-D16, shows a quite large difference compared to the other discussed curves. The anchor length for this one is 128 mm, which is significantly larger. Now there is only 34 mm CLT left between the end of the screw and the internal surface, compared to 60 mm in the three other cases. So, it appears that the main influential parameter for the heat flow is rather the remaining CLT thickness than the anchor length or the screw diameter. However, the purpose of these graphic results is mainly to get a global idea of the influence of the connections. Therefore, it is necessary to calculate some specific values, like the thermal transmittance of the internal surface temperatures, look more into detail.

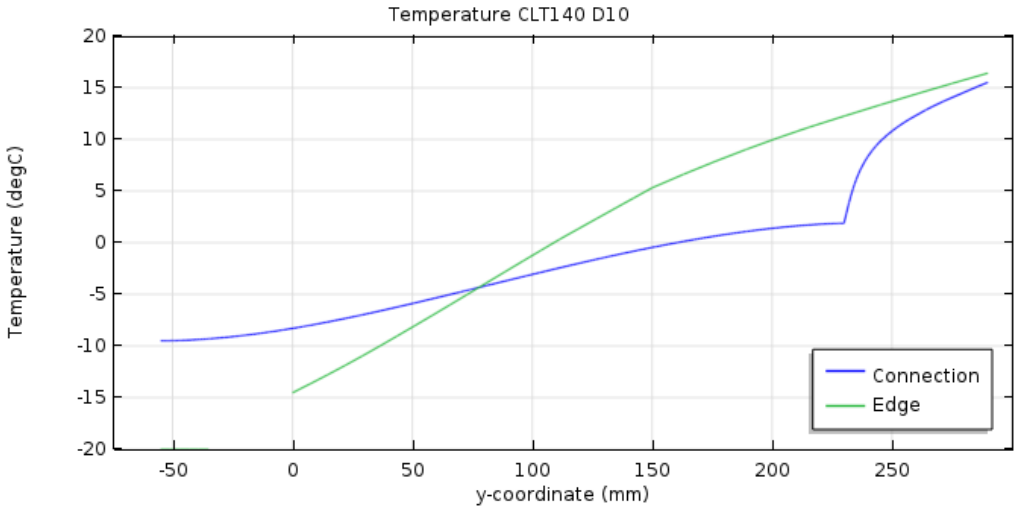

Figure 38 – Temperature curve for CLT140-D10

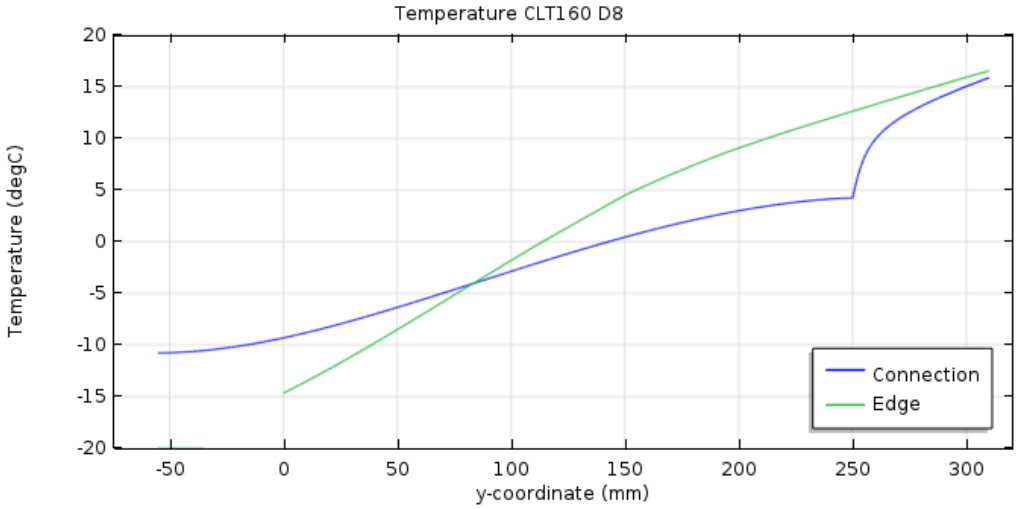

Figure 39 – Temperature curve for CLT160-D8

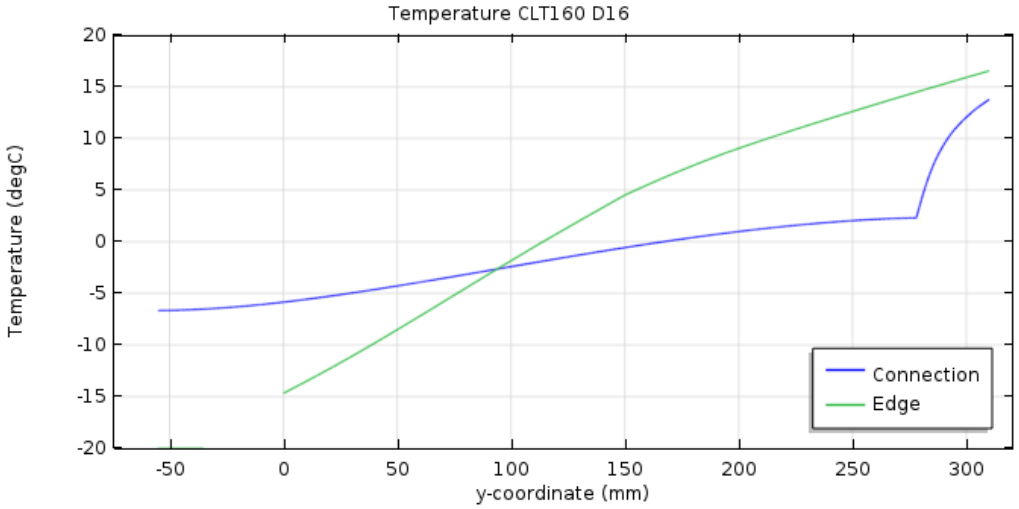

Figure 40 – Temperature curve for CLT160-16

3.4.2 Thermal transmittance

The best-known method to evaluate the thermal performances of a façade is the thermal transmittance of the structure, better known as the U-value and is expressed in W/m^{2}K. The U-value corresponds to the amount of heat that is transferred through a structure with an area of 1 m^2 for a temperature difference of 1 K between the two boundaries of that structure.

$$U = \frac{\phi}{A.\Delta T}\ [\frac{W}{m^2K}] \tag{14}$$

In this equation is ϕ known as the heat transfer or the heat flux. The thermal transmittance is a general method to express the thermal performances of a boundary structure, like a wall or a roof. The lower the U-value, the better the structure is insulated and the less heat losses. Every country has its own guidelines and requirements on this value for new buildings. The national requirements for façades in Belgium dictate a maximum U-value of $U_{max,BE} = 0{,}24\ W/m^2K$ [21], for Finland the national requirements are slightly stricter, namely $U_{max,FI} = 0{,}17\ W/m^2K$ [22].

The U-value is often calculated as:

$$U = \frac{1}{R_T} \tag{15}$$

R_T is the total thermal resistance of a structure and is the sum of the thermal resistances of each layer of the structure and the surface resistances $R_{S,i}$ and $R_{S,e}$. The thermal resistance of a certain material layer is calculated by dividing the thickness of the layer d with the thermal conductivity of that layer λ.

$$R_T = R_{S,i} + \sum \frac{d}{\lambda} + R_{S,e}\ [\frac{m^2K}{W}] \tag{16}$$

EN ISO 6946:2007 [17] states that besides equation (15), the U-value should be calculated with keeping certain corrections in mind. There are corrections for air voids in insulation, for precipitation on inverted roofs and for mechanical fasteners penetrating an insulation layer. In this study, the U-value (considering the corrections) will be calculated by using Comsol. However, it's not possible to get a U-value as output from Comsol, but it is possible to obtain the heat flux. Then it's not difficult to calculate the U-value by using equation (14).

Table 6 shows the results for the 1 x 1 m^2 models. It appears that all models fulfil both the national requirements for Belgium and Finland. To compare the different models to each other, the results have been visualised in Figure 41.

Table 6 – Calculated U-values for 1 x 1 m^2 models

	$\phi[W]$	$U\ [W/m^2K]$
CLT140-CL	6,7640	0,1691
CLT140-B	6,5681	0,1642
CLT140-D8	6,6852	0,1671
CLT140-D10	6,7149	0,1679
CLT140-D12	6,7575	0,1689
CLT160-B	6,3702	0,1593
CLT160-D8	6,4890	0,1622
CLT160-D10	6,5211	0,1630
CLT160-D12	6,5503	0,1638
CLT160-D16	6,6358	0,1659

What immediately stands out is the better performance of the thicker CLT160 panels. It is quite striking that CLT160-D12 has a lower U-value than a CLT140 panel without any connection (CLT140-B). However, the differences appear on a very low level ($10^{-3}\ W/m^2K$). According to EN ISO 6946 the U-value can be rounded to two significant figures, which means that most models lie around a U-value of 0,16 W/m²K. So, it seems that the screw diameter or CLT thickness has a rather small influence on the U-value.

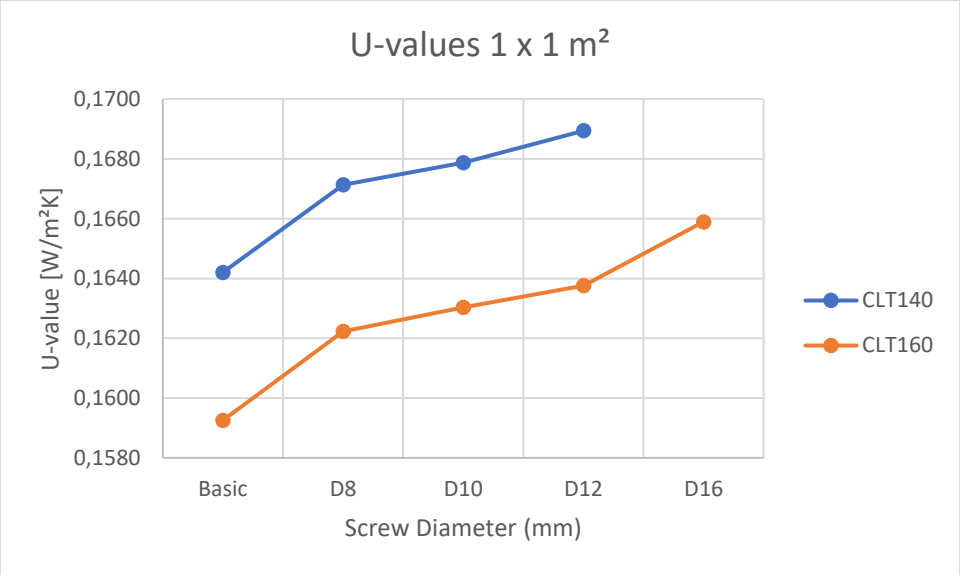

Figure 41 – Comparison of calculated U-values for 1 x 1 m^2 models

The U-values for the bigger models with 3 x 4 m^2 panels are calculated in the same way by using equation (14) on the heat flux, obtained from Comsol. Before doing these, it was suspected that the heat flux of the 3 x 4 m^2 models would simply be the sum of the heat fluxes of the 1 x 1 m^2 models:

$$\phi^* = 10.\phi_{CLT140-B} + 2.\phi_{CLT140-D8} \quad (17)$$

The results, shown in Table 7, confirm this suspicion. The difference Δ between the heat flux calculated by Comsol (U) and the value calculated by equation (17) is below 1%, which means that the difference can be neglected [18]. This means that the same principle could be applied for panels of different dimensions to calculate the heat flux (and thus the U-value) based on the 1 x 1 m^2 models. However, it doesn't seem necessary to do this because here again the U-values don't change a lot in function of the connection.

Table 7 – Calculated U-values for 3 x 4 m^2 models

	$\phi\ [W]$	$U\ [\frac{W}{m^2K}]$	$\phi^*\ [W]$	$U^*\ [\frac{W}{m^2K}]$	Δ [%]
CLT140-3x4-2D8	79,1740	0,1649	79,0514	0,1647	0,15%
CLT140-3x4-2D10	79,2310	0,1651	79,1108	0,1648	0,15%
CLT140-3x4-2D12	79,3180	0,1652	79,1960	0,1650	0,15%
CLT160-3x4-2D8	76,7930	0,1600	76,6800	0,1598	0,15%
CLT160-3x4-2D10	76,8550	0,1601	76,7442	0,1599	0,14%
CLT160-3x4-2D12	76,9130	0,1602	76,8026	0,1600	0,14%
CLT160-3x4-2D16	77,0840	0,1606	76,9736	0,1604	0,14%

Since it is already clear that the connection has almost no influence on the heat flux or U-value of the model, it doesn't seem necessary to calculate these values for the floor/wall joint model. The heat flux is a global parameter of the structure, while the connection that penetrates the façade has a local effect on the structure. That is why it's difficult to compare the different models based on the U-value. This means that it is necessary to look at local parameters, e.g. the internal surface temperature.

3.4.3 Internal surface temperature

The temperature curves from 3.4.1 show that the connections have a certain influence on the internal surface temperature. As discussed before, it seems that the remaining CLT thickness after the screw affects the magnitude of the temperature. Since, the temperature curves were obtained by defining a cut line through the screw, the received value only defines the temperature near the position of the connection. To get an overview of the surface temperature on the whole element, the temperature distribution on the internal surface has been plotted and the maximum and minimum values of the surface temperature are shown (resp. $T_{s,i,\max}$ and $T_{s,i,min}$). These plots can be found in Annex B. It is important to note that all these plots use different colour grading, depending on the range of the maximum and minimum values. The visualisation has been done this way to make the influence of the connection visible compared to the rest of the panel. The consequence of this representation is that it's not possible to visually compare the different models with each other. But the temperature values can be compared without any difficulties.

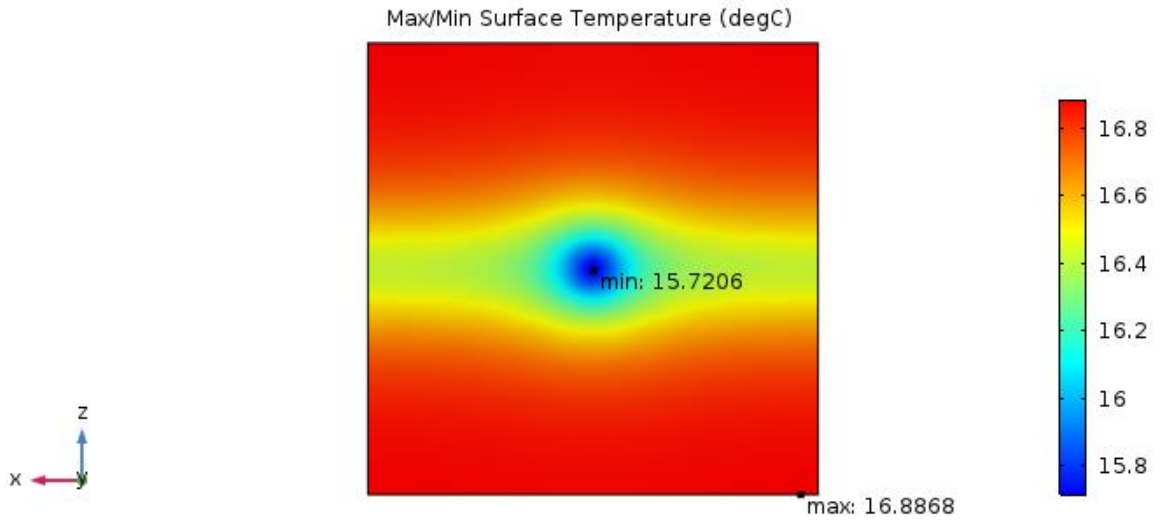

Figure 42 - Internal surface temperature CLT140-D8

Figure 42 shows the internal surface temperature distribution of the CLT140-D18 model. As expected the area near the position of the connection is colder than the rest of the panel. It is also noteworthy to mention that the influence of the timber frame is visible on the figure, but the effect of this is very low. Figure 66 of Annex B, which shows CLT140-B, visualises this effect even more, but the temperature difference is only 0,4 °C. The minimum surface temperatures of the different 1 x 1 m^2 models are compared and shown in Figure 41. This time, the difference between CLT140 and CLT160 is rather small, but as expected has CLT160 higher temperatures than CLT140. The minimum temperature for CLT160-D16 is very low compared to the other models (almost 3°C difference compared to CLT160-B).

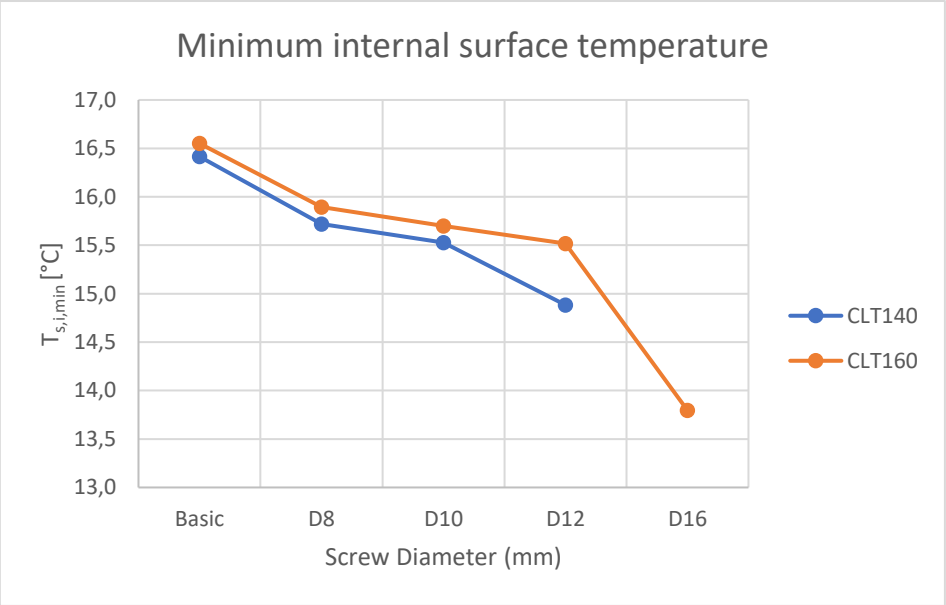

Figure 43 – Comparison of minimum surface temperature for 1 x 1 m^2 models

Figure 44 shows the surface temperature for CLT140-3x4-2D8 and confirms previous conclusions that the bigger panels are merely a collection of different small panels (see 3.4.2) because the values for $T_{s,i,\max}$ and $T_{s,i,min}$ are almost the same of CLT140-D8.

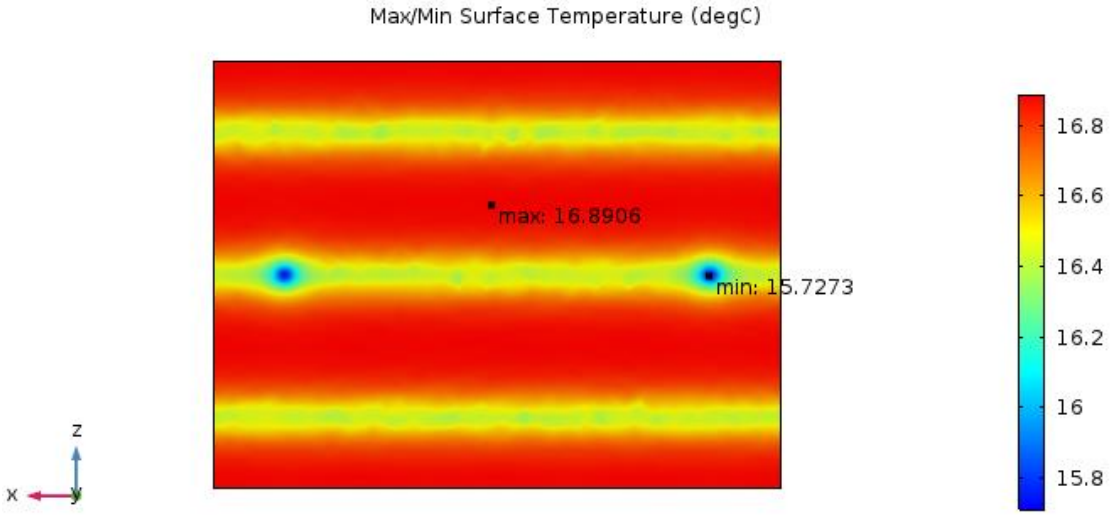

Figure 44 - Internal surface temperature CLT140-3x4-2D8

As discussed in 3.2, the floor/wall joint has been simulated in seven different models. When comparing the models with the steel barrier (Figure 45 and Figure 46) to the model without the barrier (Figure 47), it is clear that the steel barrier has a larger influence on the minimum temperature than the connections have. That's why the other models were simulated without the steel barrier, so that it's clearer to investigate the effect of the connections. Next, the position of the connections was investigated. To do this, three models were made without the steel barrier. The first one (Figure 47) has the connections at the edge of the cladding panel, as designed by

Gasparri et al. [5], the other two models have the connections on either 0,5 m or 1,0 m distance from the floor slab (resp. Figure 48 and Figure 49). The first observation is that the difference between the offset models is not that large. Both minimum temperatures are almost of the same size. This brings us to the second observation: the lowest temperatures are still situated at the joint of the floor and the wall (and not near the connection). Although, it's notable that the temperature near the connections is of the same magnitude. Thirdly, the temperature at the joint is colder for F/W-no_barrier. This means that the presence of a connection close to the joint increases the heat transfer through the joint. So, it seems that the heat transfer through the joint is equally important than the heat transfer through the connections (even more important if there's a steel barrier).

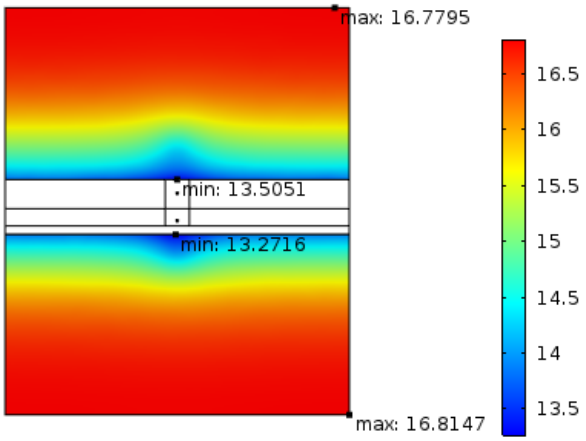

Figure 45 - Internal surface temperature F/W-barrier_CLT

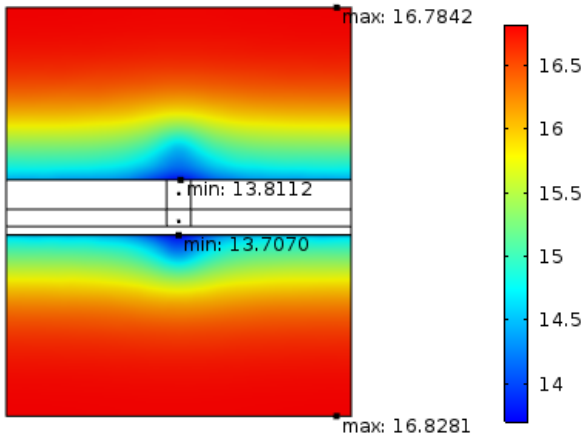

Figure 46 - Internal surface temperature F/W-barrier_ins

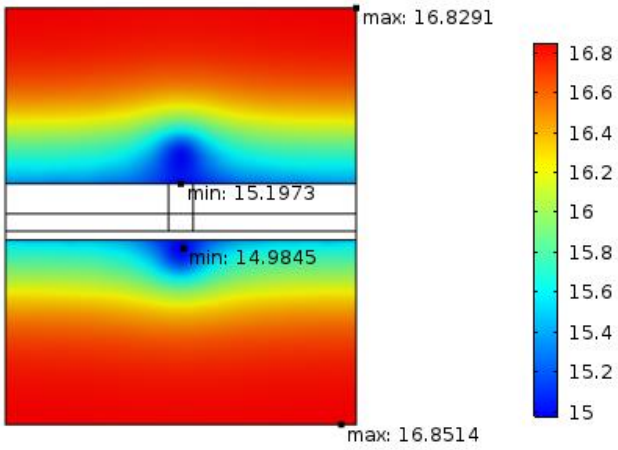

Figure 47 - Internal surface temperature F/W-no_barrier

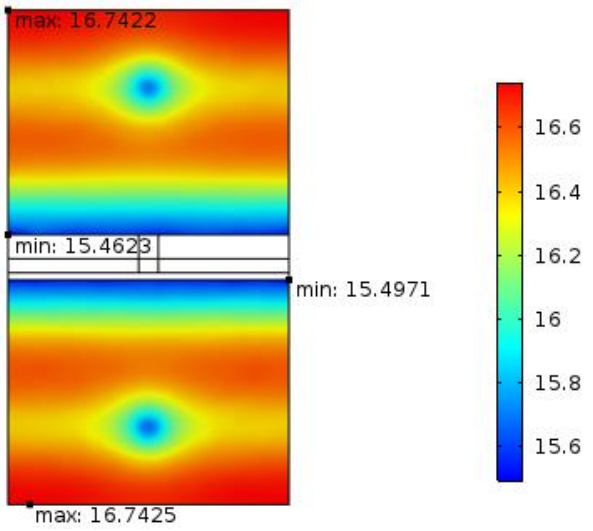

Figure 48 - Internal surface temperature F/W-conn_0.5

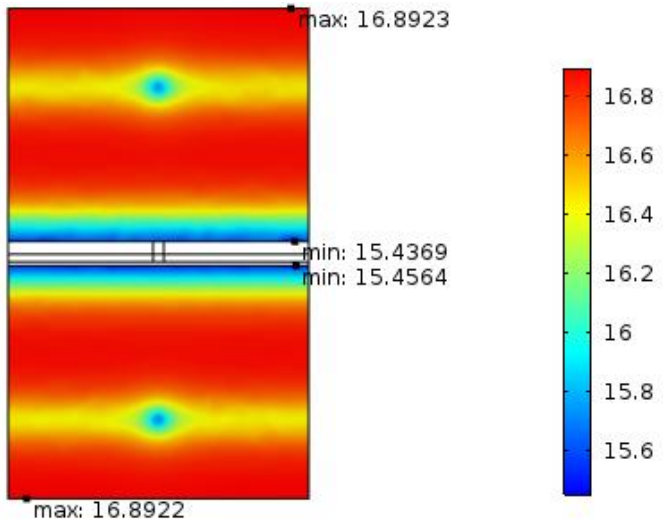

Figure 49 - Internal surface temperature F/W-conn_1.0

There was also one model simulated without steel barrier and without any connections (Annex B, Figure 87). But it seems that this just produces the same results from the model with connections on an offset of 1,0 m.

To check the importance of the horizontal joint design of the Gasparri-model, another model was simulated with a complete different build-up (Figure 50). The results of this model are shown in Figure 51. It is immediately clear that the heat transfer near the joint is larger than the original model and is relatively larger than the heat transfer near the connections.

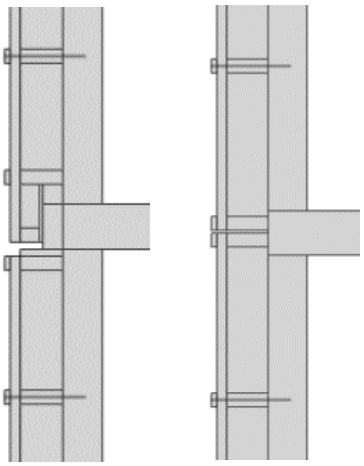

Figure 50 – F/W-conn_0.5 build-up (left) vs. F/W-diff build-up (right)

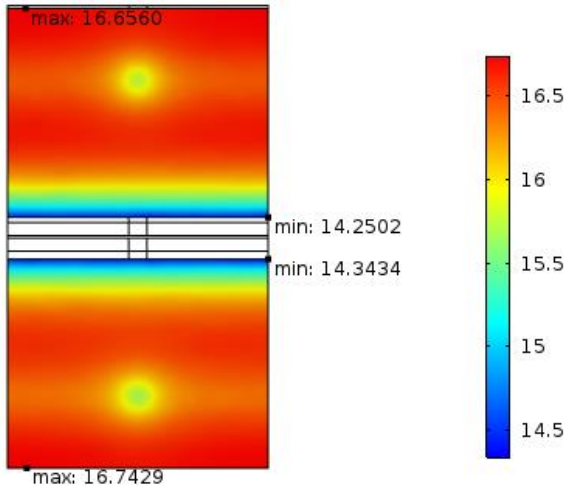

Figure 51 - Internal surface temperature F/W-diff

The minimum surface temperatures of the different floor/wall joint models are compared and shown in Figure 52. Since all the F/W models have a CLT wall thickness of 140 mm and screws of 8 mm, the value of CLT140-D8 has also been plotted as a reference. As mentioned above, the minimum temperatures for these models are all positioned near the joint. So, this reference line could be interpreted as the temperature near the position of the connection.

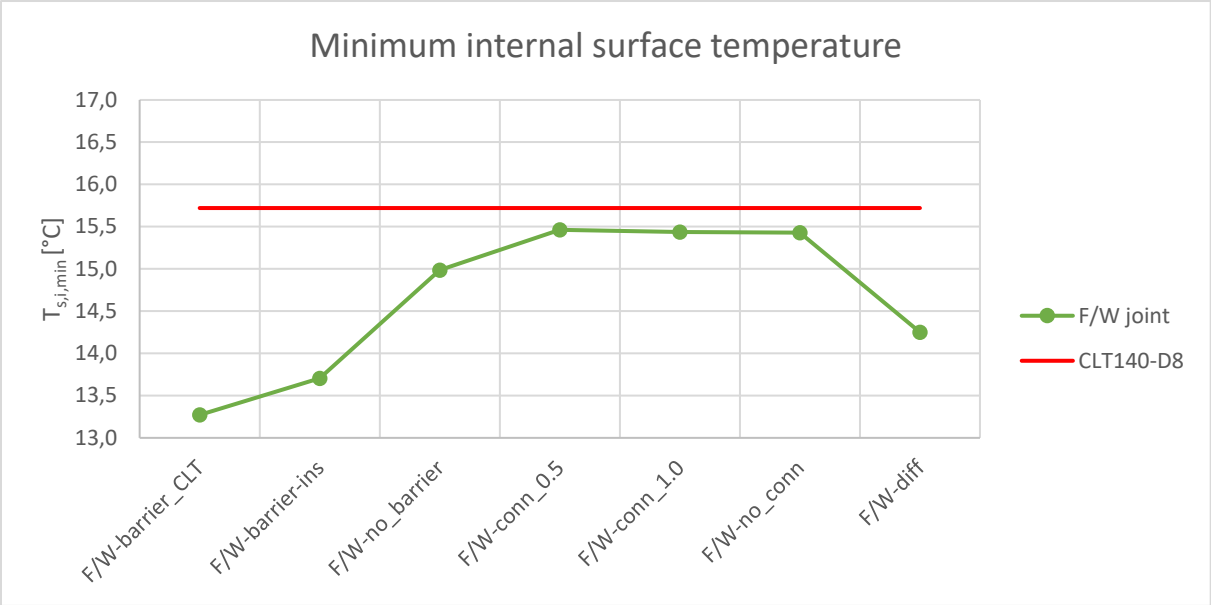

Figure 52 – Comparison of minimum internal surface temperature for F/W joint models

All the results for the internal surface temperatures are shown in Table 10 on page 42. The results for the F/W models are divided in the upper part and the lower part of the wall (resp. marked as U and L).

3.4.4 Discussion of the results

Now that all these values for the internal surface temperature are obtained, it is time to check the consequences. Since the thermal performance (U-value) of the façade is barely effected by the presence of the connections, perhaps they have consequences for surface condensation risk or cause local discomfort for people standing near the external wall.

When a surface reaches a critical surface humidity, it can lead to surface condensation and consequently to problems like mould growth. Therefore, there should be a minimum internal surface temperature to prevent that this critical surface humidity is reached. According to EN ISO 13788:2012 [23], the condensation risk on the internal surface of a structure can be evaluated by the temperature factor at the internal surface f_{Rsi}, also called thermal quality or temperature ratio. The temperature factor shows the relation between the total thermal resistance of the building envelope R_T to the thermal resistance of the building envelope without the internal surface resistance R_{si} [24].

$$f_{Rsi} = \frac{R_T - R_{si}}{R_T} \; [-] \tag{18}$$

The temperature ratio can also be calculated by taking the difference between the temperature of the internal surface and the external air temperature, and dividing it by the difference between indoor and outdoor air temperature:

$$f_{Rsi} = \frac{T_{si} - T_e}{T_i - T_e} \tag{19}$$

Each country has its different national requirements for this temperature factor. In Belgium, the temperature factor should be $f_{Rsi} \geq 0{,}70$. In Finland, they make a distinction between external walls in general ($f_{Rsi} \geq 0{,}87$) and near junctions of the thermal envelope or near penetrations of the thermal envelope ($f_{Rsi} \geq 0{,}65$) [24]. So, let's say that the temperature ratio should be more than 0,70. The calculated temperature factors for the models can be found in Table 10 on the end of this chapter. According to the table, the temperature ratio for all models lies far above the value of 0,70. So it is safe to say that there is no risk for surface condensation.

However, it could be possible that people who are standing close to the external wall experience local thermal discomfort. EN ISO 7730:2005 [25] explains the correct methods to verify thermal comfort. Thermal comfort is a very subjective factor and depends on the personal experience of people. The thermal sensation of a person is related to the thermal body balance and is influenced by physical activity and clothing, as well as environmental parameters like air temperature, mean radiant temperature, air velocity and air humidity.

The code mentions two statistical models to describe thermal comfort. The first is the PMV model, or the predicted mean vote method, and uses a thermal sensation scale that ranges from -3 cold to +3 hot (see Table 8).

Table 8 – PMV thermal sensation scale

+3	Hot
+2	Warm
+1	Slightly warm
0	Neutral
-1	Slightly cool
-2	Cool
-3	Cold

While the PMV predicts the mean thermal vote of people exposed to the same environment, the individual votes are spread out around this mean value. Therefore, there is a second statistical model: the PPD model, or the predicted percentage dissatisfied method. The PPD gives a prediction of the percentage of people that are thermally dissatisfied (uncomfortably *warm*, *hot*, *cool* or *cold*). Figure 53 shows the relation between PPD and PMV. It's important to note that even if the mean thermal vote has a value of 0, there will always be 5% of the people that is dissatisfied.

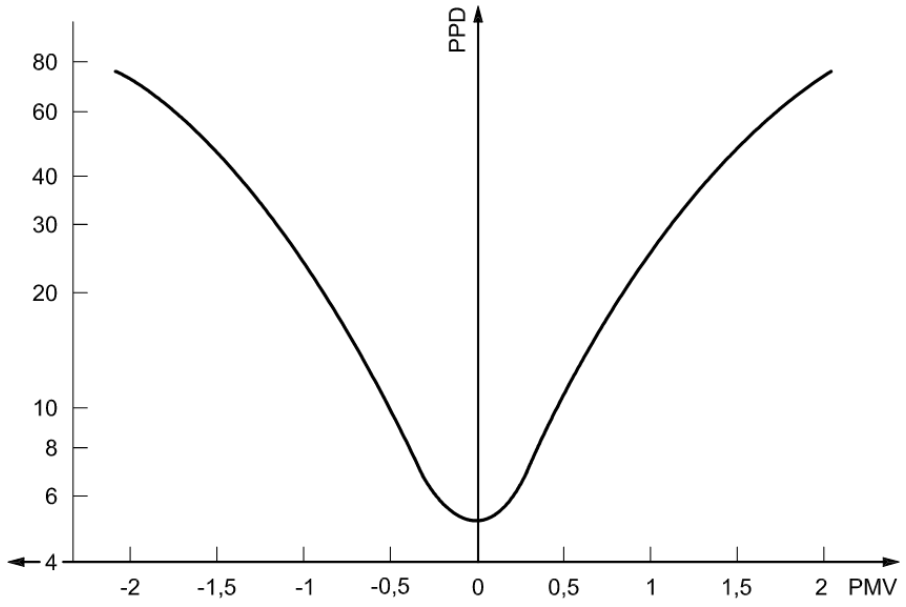

Figure 53 – PPD as function of PMV [25]

Thermal discomfort can also be caused by unwanted cooling/heating of one particular part of the body, also called local discomfort. Different causes of local discomfort could be draught, but also vertical temperature difference or radiant asymmetry. For this study, the last two causes are relevant.

If there is a high vertical temperature difference between head and ankles, people experience local discomfort. EN ISO 7730:2005 provides an equation and graph (Figure 54) to calculate the percentage dissatisfied (PD) for the vertical temperature difference:

$$PD_v = \frac{100}{1 + \exp(5{,}76 - 0{,}856.\Delta T_v)}\ [\%] \tag{20}$$

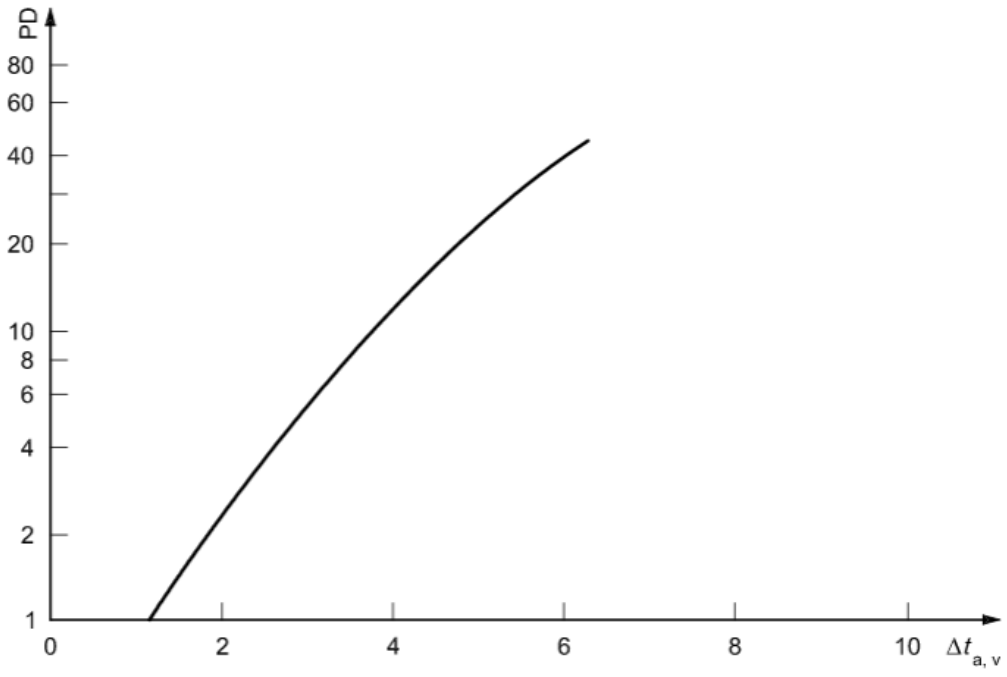

Figure 54 – Local discomfort by vertical temperature difference [25]

The vertical temperature difference of the simulated models has been calculated by taking the difference between the maximum and minimum internal surface temperature.

$$\Delta T_v = T_{s,i,max} - T_{s,i,min} \tag{21}$$

The second relevant cause for thermal discomfort is radiant asymmetry. This happens for example when walls are cooler than the rest of the room. The percentage dissatisfied for radiant asymmetry is calculated with the following equation and is visualised on line 2 of Figure 55.

$$PD_r = \frac{100}{1 + \exp(9{,}93 - 0{,}50.\Delta T_r)}\ [\%] \tag{22}$$

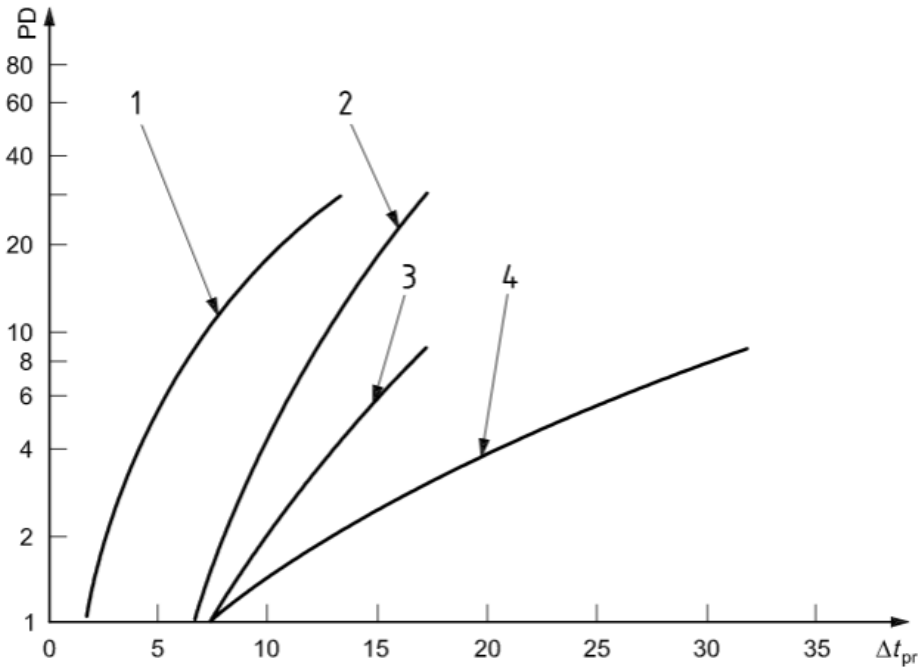

Figure 55 – Local discomfort by radiant temperature asymmetry [25], line 2 for cool walls

The radiant temperature asymmetry of the simulated models has been calculated by taking the difference between the internal air temperature ($20°C$) and the minimum internal surface temperature.

$$\Delta T_r = T_i - T_{s,i,min} \tag{23}$$

According to EN ISO 7730:2005, thermal comfort can be classified in three categories A, B and C (see Table 9). Each category describes a maximum percentage PPD and a maximum PD for local discomfort.

Table 9 – Categories of thermal comfort [25]

Category	Thermal state of the body as a whole		Local discomfort			
	PPD %	PMV	DR %	PD % caused by		
				vertical air temperature difference	warm or cool floor	radiant asymmetry
A	< 6	− 0,2 < PMV < + 0,2	< 10	< 3	< 10	< 5
B	< 10	− 0,5 < PMV < + 0,5	< 20	< 5	< 10	< 5
C	< 15	− 0,7 < PMV < + 0,7	< 30	< 10	< 15	< 10

The results for local discomfort are shown in Table 10. The results show that most of the simplified models are categorized in cat. A. But it is more relevant to look at the floor/wall joints, because the defining factor is the vertical temperature difference and people standing near the wall will stand near the joint. It seems that the models with the fire barrier are categorized in lower categories (B or C). The other models were just modelled without the steel barrier to investigate the connections, but in reality they have fire barriers too. So, the other F/W models would also have category B or C. However, that doesn't mean that this is a big problem for thermal comfort. The PMV for category C is still below +/- 0,7 and there are less than 15% of the people dissatisfied. But it is good to remember that thermal comfort must be considered.

To summarize, the presence of connections has very little to no influence on the U-value of the façade. They do have a certain effect on the internal surface temperature, but this effect is equally important as the floor/wall joint (and the presence of a steel fire barrier). The only factor that needs attention is the local thermal discomfort caused by the vertical temperature difference. But for the rest, there is no indication that the build-up suggested in this study can't be applied.

Table 10 – Results for internal surface temperatures

		$T_{s,i,max}$ [°C]	$T_{s,i,min}$ [°C]	$f_{R,s,i}$ [−]	ΔT_v [°C]	ΔT_r [°C]	PD_v [%]	PD_r [%]	$Cat.$
CLT140-B		16,8864	16,4154	0,91	0,47	3,58	0,47	0,46	A
CLT140-D8		16,8868	15,7206	0,89	1,17	4,28	0,85	0,59	A
CLT140-D10		16,8858	15,5291	0,89	1,36	4,47	1,00	0,63	A
CLT140-D12		16,8858	14,8834	0,87	2,00	5,12	1,72	0,78	A
CLT160-B		16,9461	16,5514	0,91	0,39	3,45	0,44	0,44	A
CLT160-D8		16,9461	15,8934	0,90	1,05	4,11	0,77	0,55	A
CLT160-D10		16,9447	15,7010	0,89	1,24	4,30	0,91	0,59	A
CLT160-D12		16,9436	15,5177	0,89	1,43	4,48	1,06	0,63	A
CLT160-D16		16,9434	13,7966	0,84	3,15	6,20	**4,45**	1,13	**B**
CLT140-3x4-2D8		16,8906	15,7273	0,89	1,16	4,27	0,85	0,58	A
CLT140-3x4-2D10		16,8896	15,5215	0,89	1,37	4,48	1,01	0,63	A
CLT140-3x4-2D12		16,8899	14,8010	0,87	2,09	5,20	1,85	0,80	A
CLT160-3x4-2D8		16,9500	15,9038	0,90	1,05	4,10	0,77	0,55	A
CLT160-3x4-2D10		16,9493	15,6841	0,89	1,27	4,32	0,92	0,59	A
CLT160-3x4-2D12		16,9488	15,5198	0,89	1,43	4,48	1,06	0,63	A
CLT160-3x4-2D16		16,9484	13,7029	0,84	3,25	6,30	**4,83**	1,17	**B**
F/W-barrier_CLT	U	16,7795	13,5051	0,84	3,27	6,49	**4,94**	1,25	**C**
	L	16,8147	13,2716	0,83	3,54	6,73	**6,14**	1,35	
F/W-barrier_ins	U	16,7842	13,8112	0,85	2,97	6,19	**3,86**	1,13	**B**
	L	16,8281	13,7070	0,84	3,12	6,29	**4,36**	1,17	
F/W-no_barrier	U	16,8291	15,1973	0,88	1,63	4,80	1,26	0,70	A
	L	16,8514	14,9845	0,87	1,87	5,02	1,53	0,75	
F/W-conn_0.5	U	16,7422	15,4623	0,89	1,28	4,54	0,93	0,64	A
	L	16,7425	15,4971	0,89	1,25	4,50	0,91	0,63	
F/W-conn_1.0	U	16,8923	15,4369	0,89	1,46	4,56	1,08	0,65	A
	L	16,8922	15,4564	0,89	1,44	4,54	1,07	0,64	
F/W-no_conn	U	16,7838	15,4299	0,89	1,35	4,57	0,99	0,65	A
	L	16,8056	15,4375	0,89	1,37	4,56	1,01	0,65	
F/W-diff	U	16,6560	14,2502	0,86	2,41	5,75	2,41	0,97	A
	L	16,7429	14,3434	0,86	2,40	5,66	2,40	0,94	

4 Conclusion

This study investigated the connections of prefabricated façade systems with a CLT substructure. In particular, the effect of large-diameter-connections on heat transfer and thermal bridging has been analysed.

The minimum required number of screws to attach the prefab cladding elements to the CLT has been calculated based on permanent loads and wind loads. The results showed that the necessary amount of screws is low as long as the cladding elements have reasonable dimensions.

Different simplified models have been simulated to retrieve a visual representation of the heat flow and to calculate the thermal transmittance of the external wall. The results show that the connections have almost no effect on the size of the U-value. But they do have a certain influence on the internal surface temperatures. Surface condensation risk won't be a problem, but local discomfort of people standing close to the wall could be an issue. The simulations also point out that the influence of the floor/wall joint is equally important – if not more important – than the connections penetrating the wall.

The conclusion of this research is that large-diameter-connections have little effect on thermal transmittance and thermal comfort. This means that it could be possible to connect cladding elements to a CLT structure with fewer connections, resulting in a higher construction speed and perhaps even the possibility to create a replaceable cladding system.

References

[1] TES EnergyFaçade. (2008-2009). Prefabricated timber based building system for improving the energy efficiency of the building envelope.

[2] Maroy, K., Van Den Bossche, N., Steeman, M., De Corte, W., & Janssens, A. (2016). *Potential of existing prefabricated components for sustainable renovation of buildings.* Paper presented at the CESB16: Central Europe towards Sustainable Building 2016.

[3] Dubois, S., Remy, O., & de Bouw, M. (2016). Retrofitting with AIM-ES - Guidelines.

[4] Gasparri, E., Lucchini, A., Mantegazza, G., & Mazzucchelli, E. S. (2015). Construction management for tall CLT buildings: From partial to total prefabrication of façade elements. *Wood Material Science & Engineering, 10*(3), 256-275.

[5] Gasparri, E., Giunta, G., Mazzucchelli, E. S., & Lucchini, A. (2016). *Prefabricated CLT façade systems for fast-track construction and quality assurance.* Paper presented at the proceedings of World Conference on Timber Engineering, Wien, Austria.

[6] Gasparri, E., Lam, F., & Liu, Y. (2016). *Compression perpendicular to grain behavior for the design of a prefabricated CLT façade horizontal joint.* Paper presented at the proceedings of World Conference on Timber Engineering, Wien, Austria.

[7] Studiengemeinschaft Holzleimbau. Building with Cross Laminated Timber. Retrieved from http://www.clt.info/en/media-downloads/brochures/brochures/

[8] Evans, L. (2013). Cross Laminated Timber. Retrieved from http://www.rethinkwood.com/sites/default/files/Cross-Laminated-Timber-CEU.pdf

[9] proHolz. (2014). Cross-Laminated Timber Structural Design - Basic design and engineering principles according to Eurocode. Vienna: proHolz Austria.

[10] StoraEnso. (2016). Technical Brochure CLT. Retrieved from http://www.clt.info/en/media-downloads/brochures/brochures/

[11] Sun, J. (2016). *Mid-rise Timber Construction in Finland: A Study on Material, Technology and Market Maturity.* Helsinki Metropolia University of Applied Sciences.

[12] WTCB. (2016). Wind Interactive. Retrieved from http://www.wtcb.be/homepage/index.cfm?cat=services&sub=standards_regulations&pag=norm_eurocodes&art=calculator

[13] EN 1991-1-4. (2005). *Eurocode 1: Actions on structures - Part 1-4: General actions - Wind actions*. Brussels: European committee for standardization.

[14] Finnish National Annex to SFS-EN 1990 Eurocode. (2007). *Basis of structural design*. Helsinki.

[15] WTCB. (2012). Fiche Eurocode EN 1991-1-4.

[16] EN 1995-1-1. (2004). *Eurocode 5: Design of timber structures - Part 1-1: General - Common rules and rules for buildings*. Brussels: European committee for standardization.

[17] EN ISO 6946. (2007). *Building components and building elements - Thermal resistance and thermal transmittance - Calculation method*. Brussels: European committee for standardization.

[18] EN ISO 10211. (2007). *Thermal bridges in building construction - Heat flows and surface temperatures - Detailed calculations*. Brussels: European committee for standardization.

[19] Comsol. Thermal Bridges in Building Construction—3D Structure Between Two Floors. Retrieved from

https://www.comsol.com/model/download/394531/models.heat.thermal_bridge_3d_two_floors.pdf

[20] Comsol. Thermal Bridges in Building Construction—3D Iron Bar Through Insulation Layer. Retrieved from https://www.comsol.com/model/download/394511/models.heat.thermal_bridge_3d_iron_bar.pdf

[21] Energiesparen.be. (2016). Maximaal toelaatbare U-waarden. Retrieved from http://www2.vlaanderen.be/economie/energiesparen/epb/doc/epbuwaarden2016.pdf

[22] ym.fi. (2017). Energy efficiency of building. Retrieved from http://www.ym.fi/en-US/Land_use_and_building/Legislation_and_instructions/The_National_Building_Code_of_Finland/Energy_efficiency_of_buildings

[23] EN ISO 13788. (2012). *Hygrothermal performance of building components and building elements - Internal surface temperature to avoid critical surface humidity and interstitial condensation - Calculation methods*. Brussels: European committee for standardization.

[24] Kalamees, T. (2006). *Critical values for the temperature factor to assess thermal bridges.* Paper presented at the Proceedings of the Estonian Academy of Sciences.

[25] EN ISO 7730. (2005). *Ergonomics of the thermal environment - Analytical determination and interpretation of thermal comfort using calculation of the PMV and PPD indices and local thermal comfort criteria*. Brussels: European committee for standardization.

Annexes

A. Temperature curves

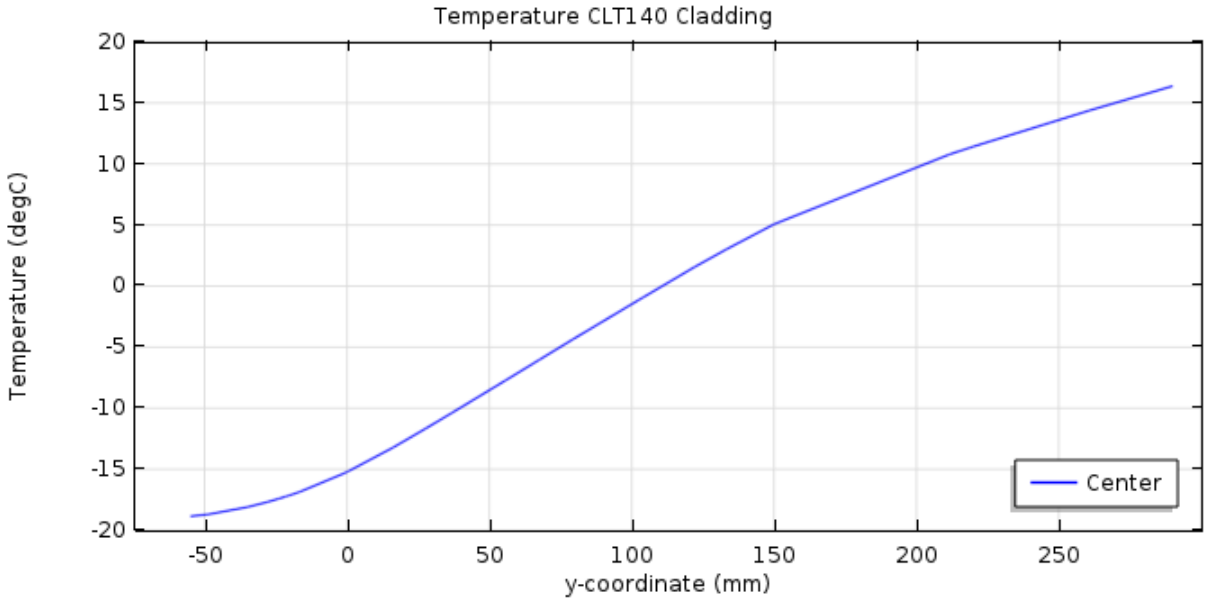

Figure 56 - Temperature curve CLT140-CL

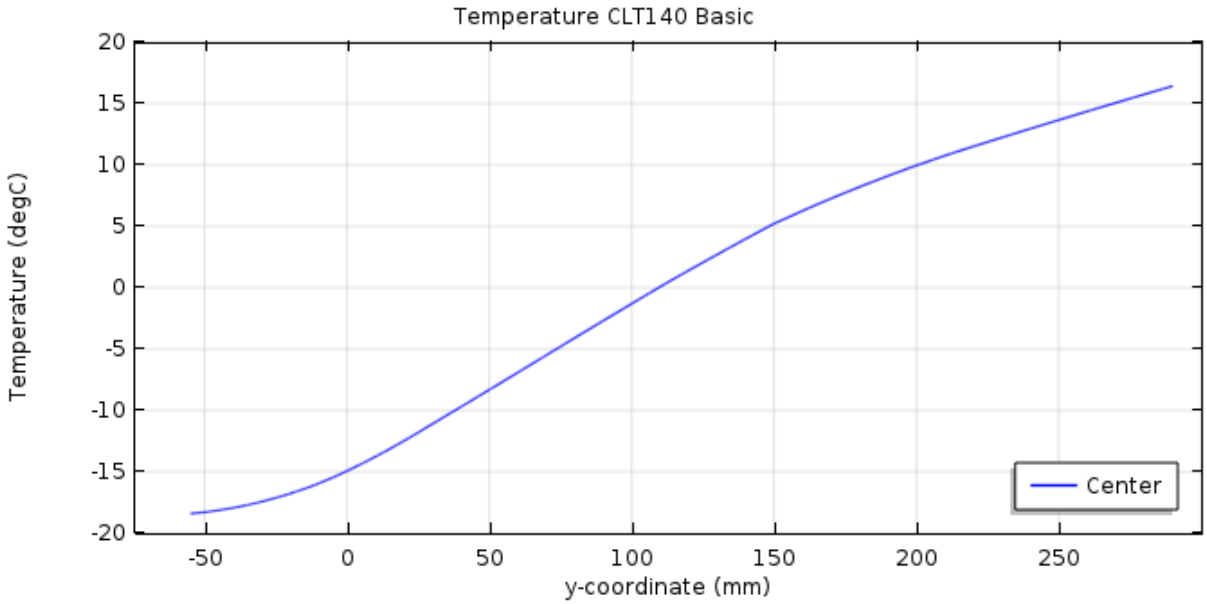

Figure 57 - Temperature curve CLT140-B

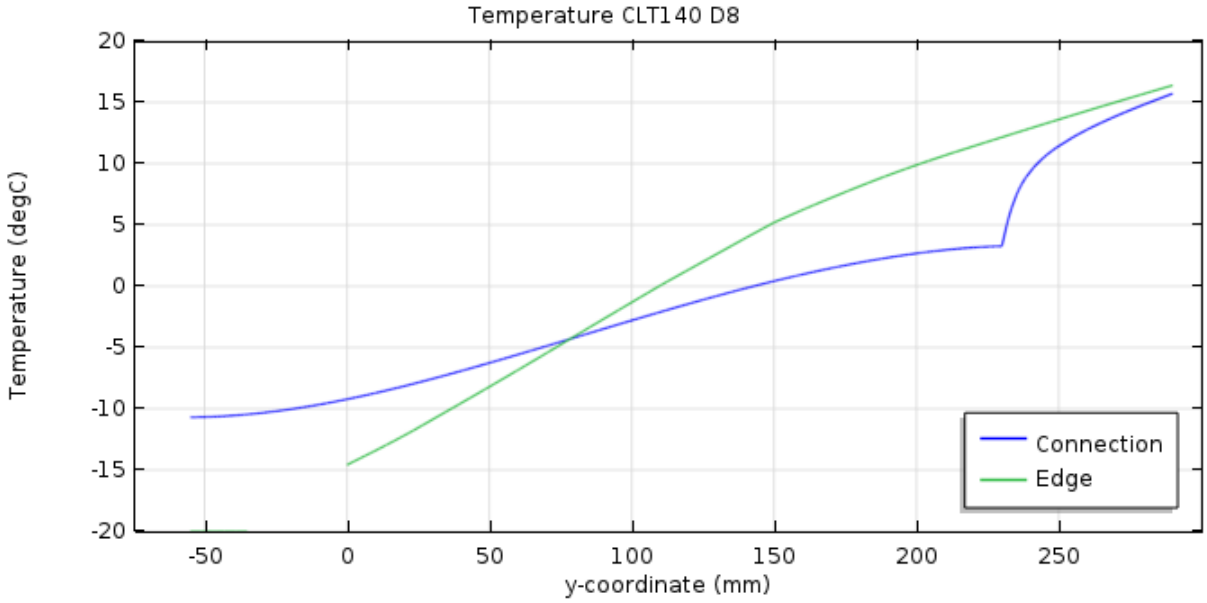

Figure 58 - Temperature curve CLT140-D8

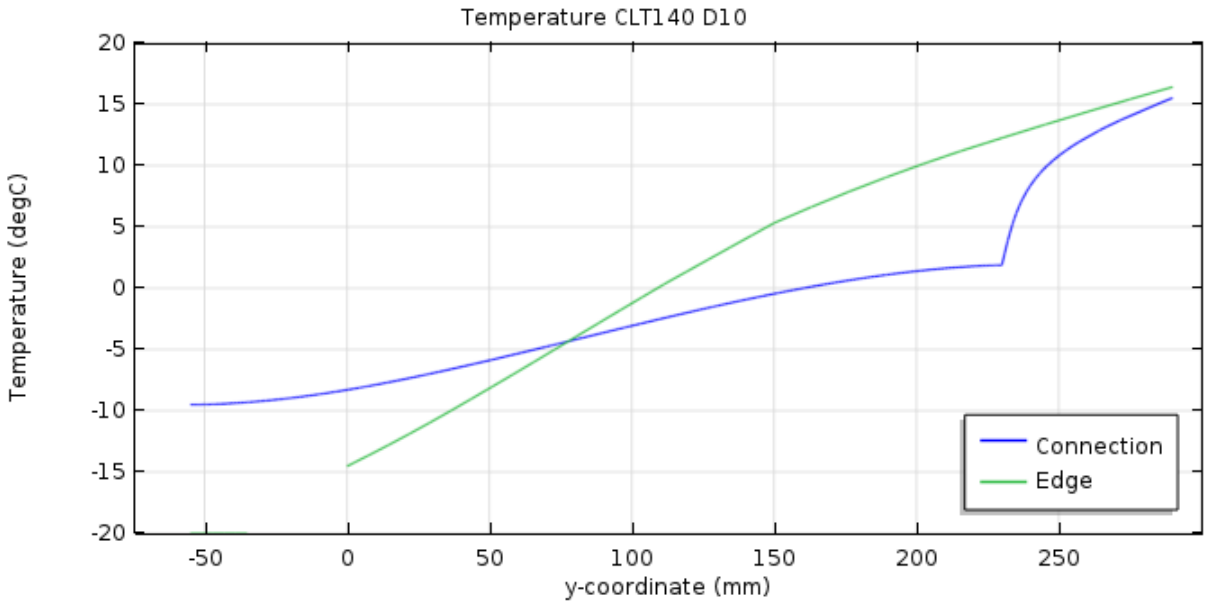

Figure 59 - Temperature curve CLT140-D10

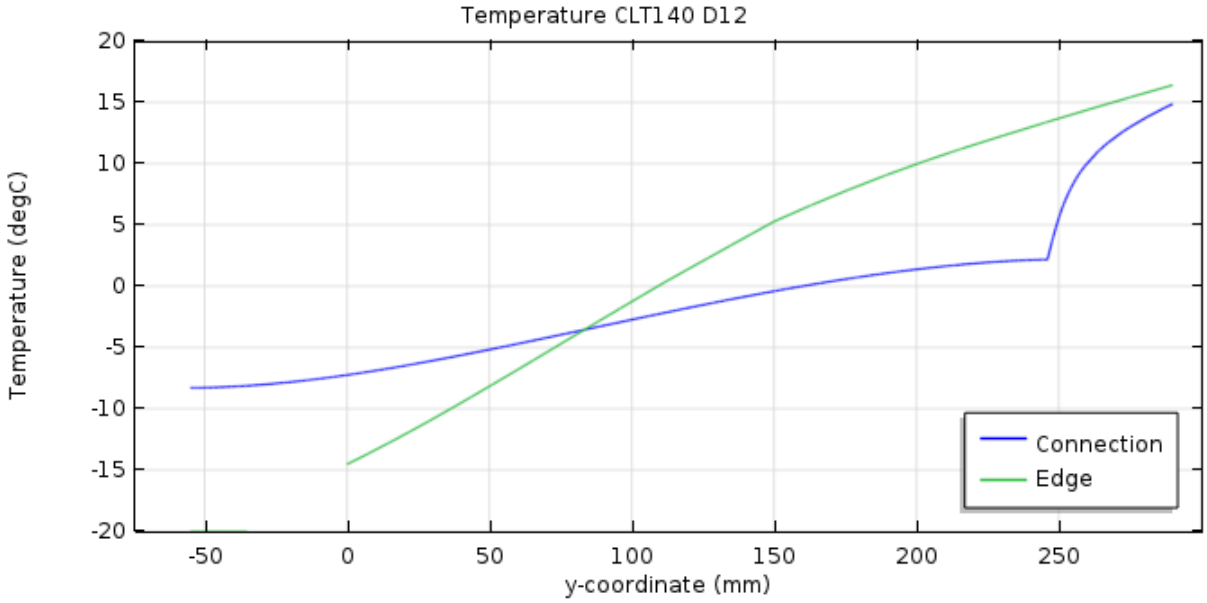

Figure 60 - Temperature curve CLT140-D12

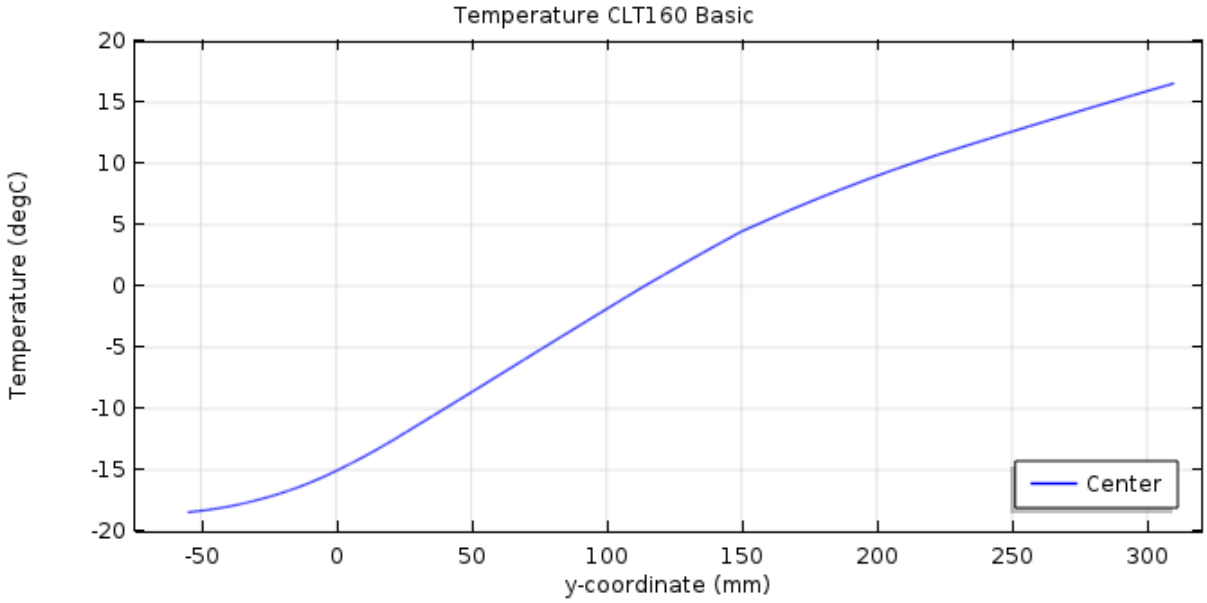

Figure 61 - Temperature curve CLT160-B

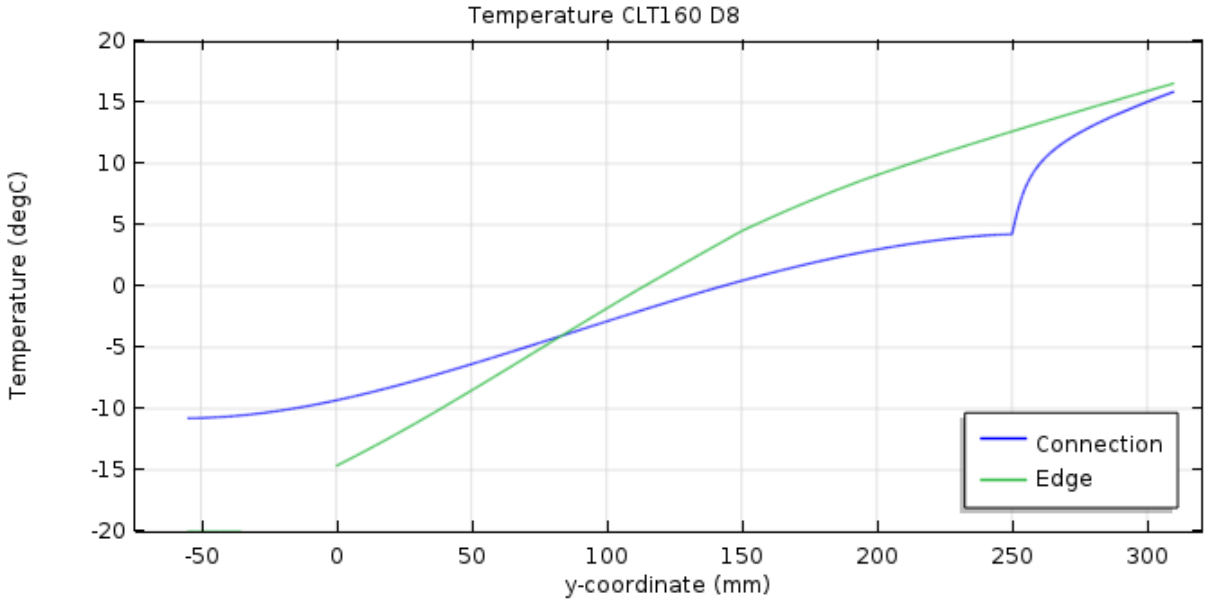

Figure 62 - Temperature curve CLT160-D8

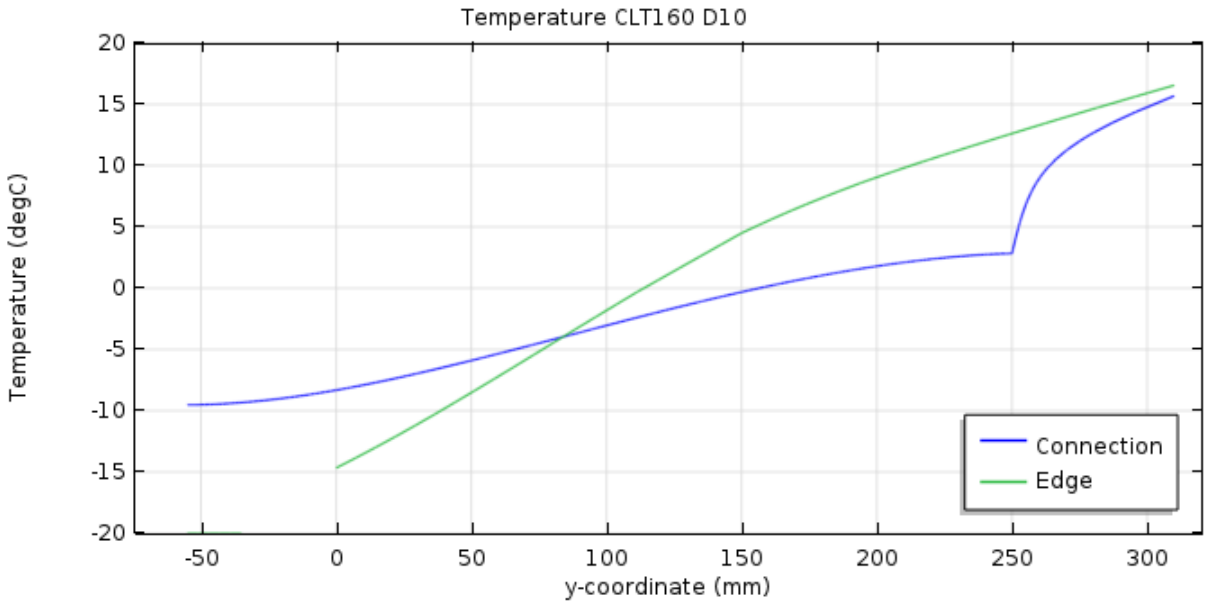

Figure 63 - Temperature curve CLT160-D10

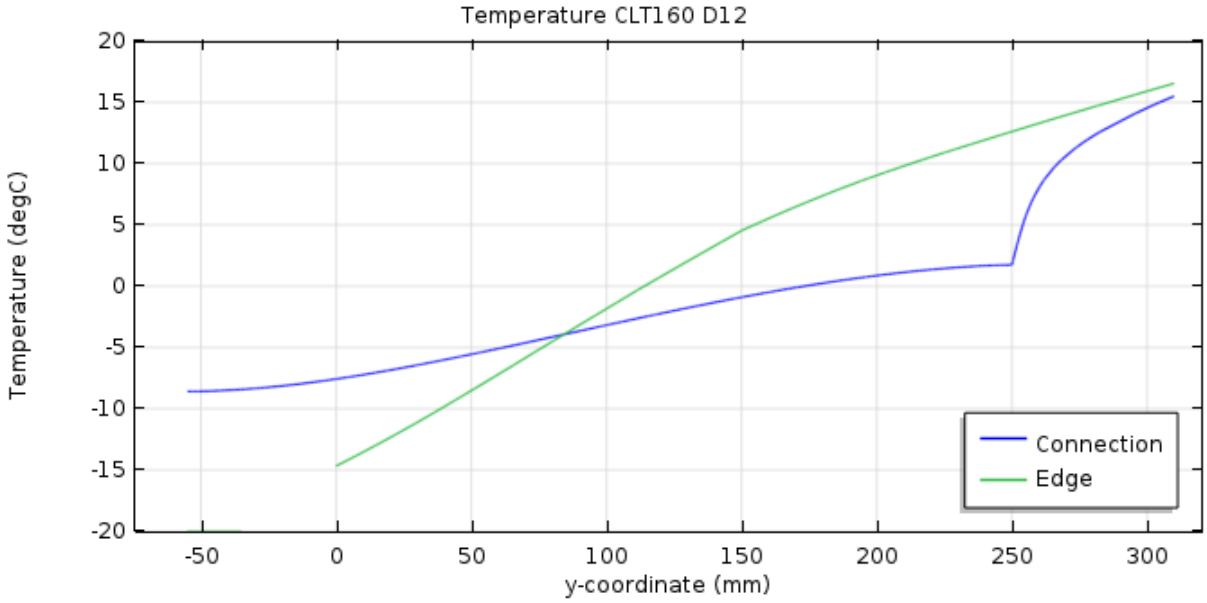

Figure 64 - Temperature curve CLT160-D12

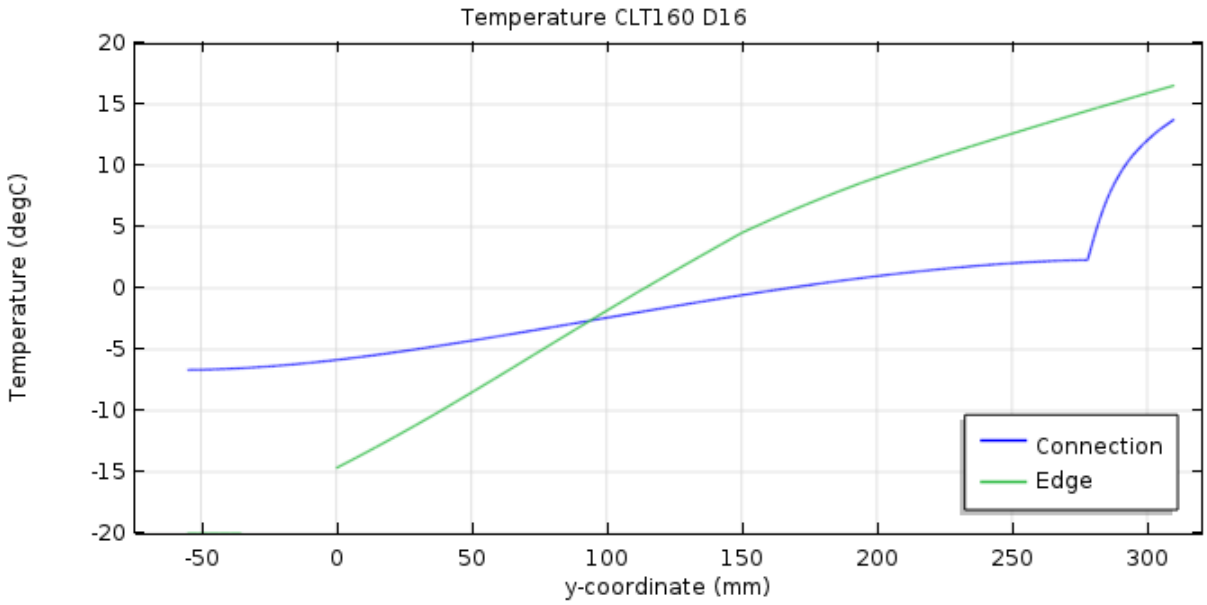

Figure 65 - Temperature curve CLT160-D16

B. Internal surface temperature distribution

Model type 1 x 1 m²

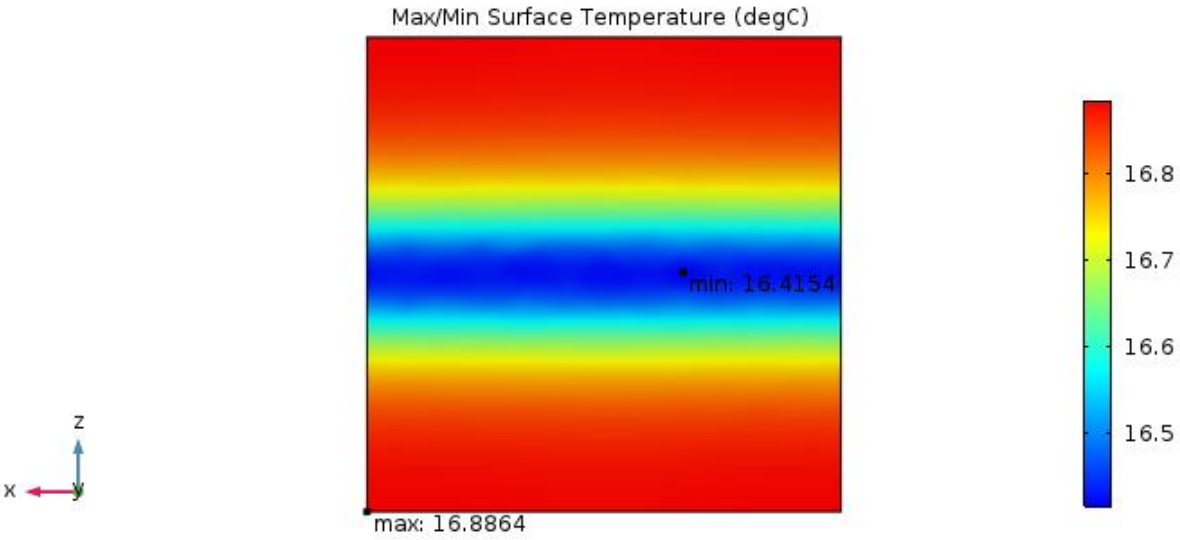

Figure 66 – Internal surface temperature CLT140-B

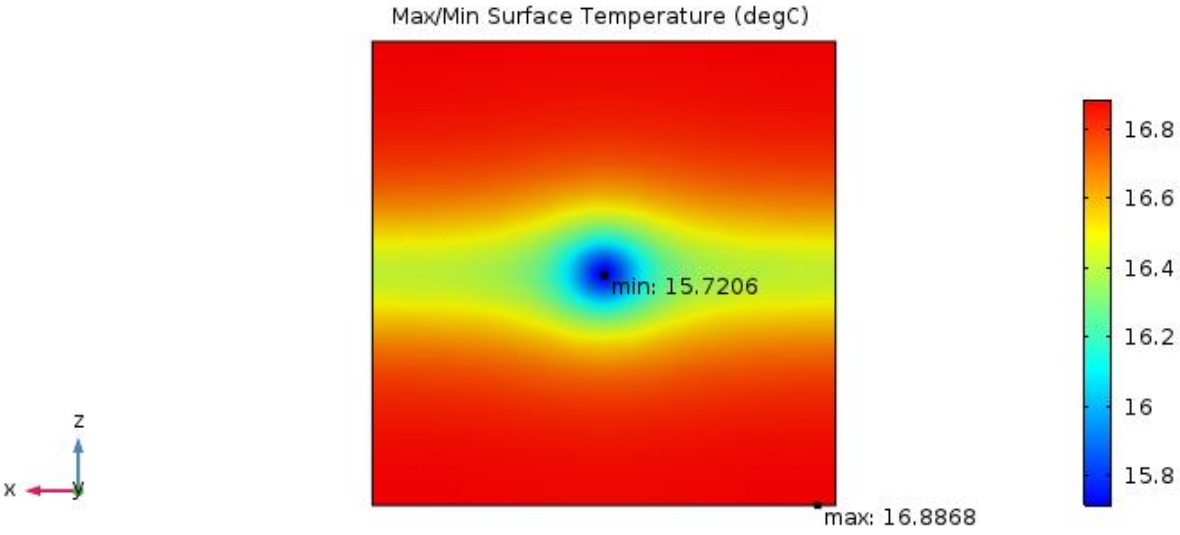

Figure 67 - Internal surface temperature CLT140-D8

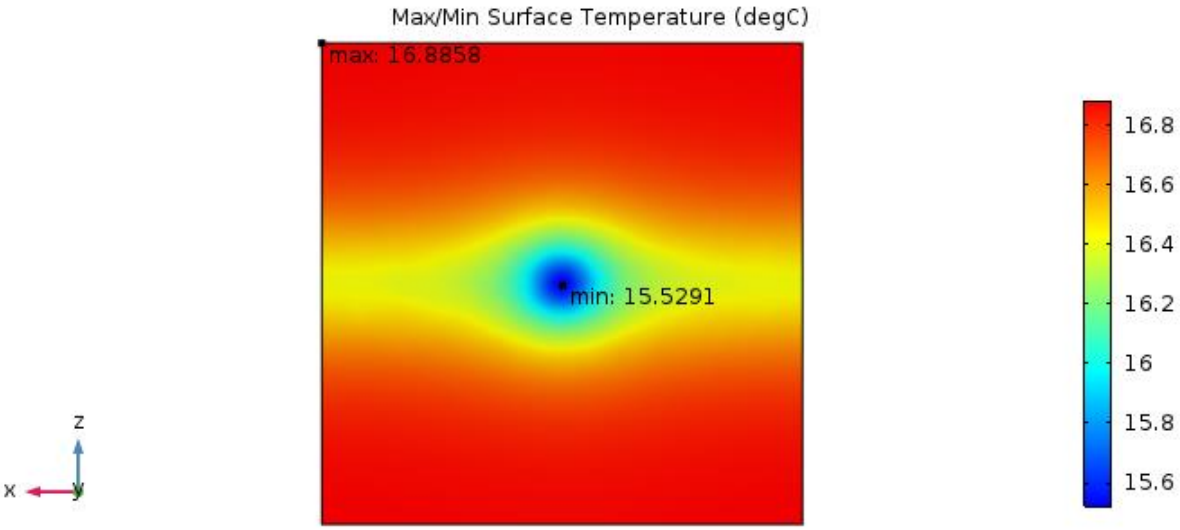

Figure 68 - Internal surface temperature CLT140-D10

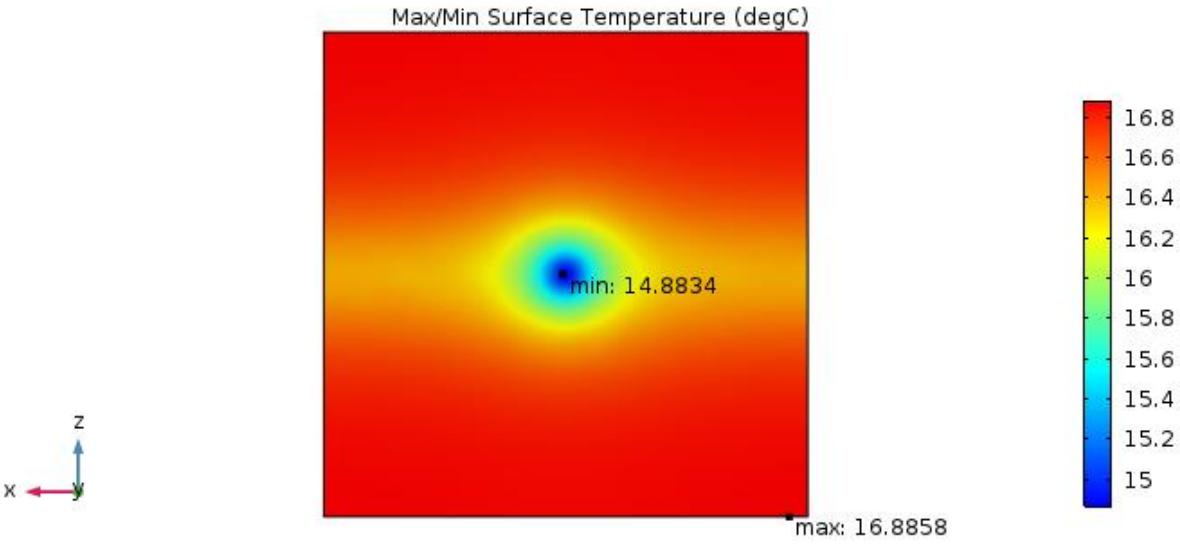

Figure 69 - Internal surface temperature CLT140-D12

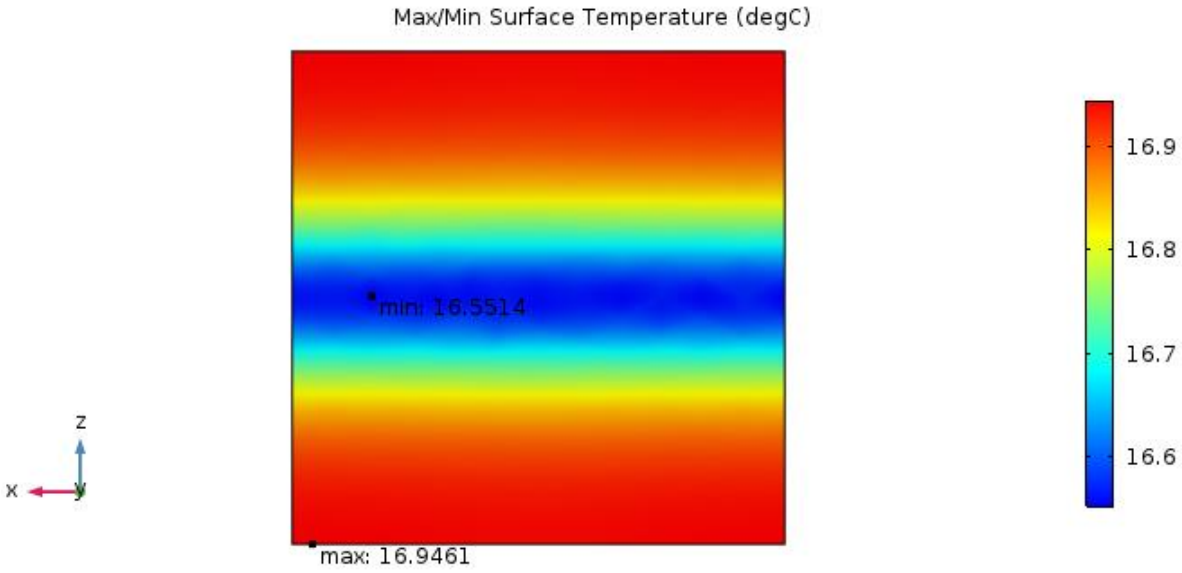

Figure 70 - Internal surface temperature CLT160-B

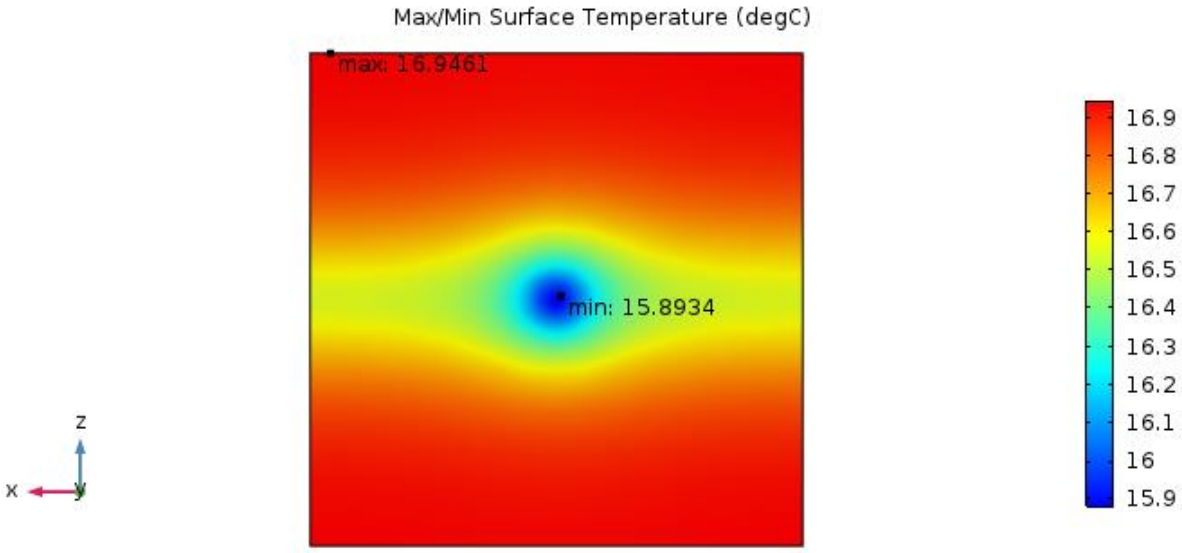

Figure 71 - Internal surface temperature CLT160-D8

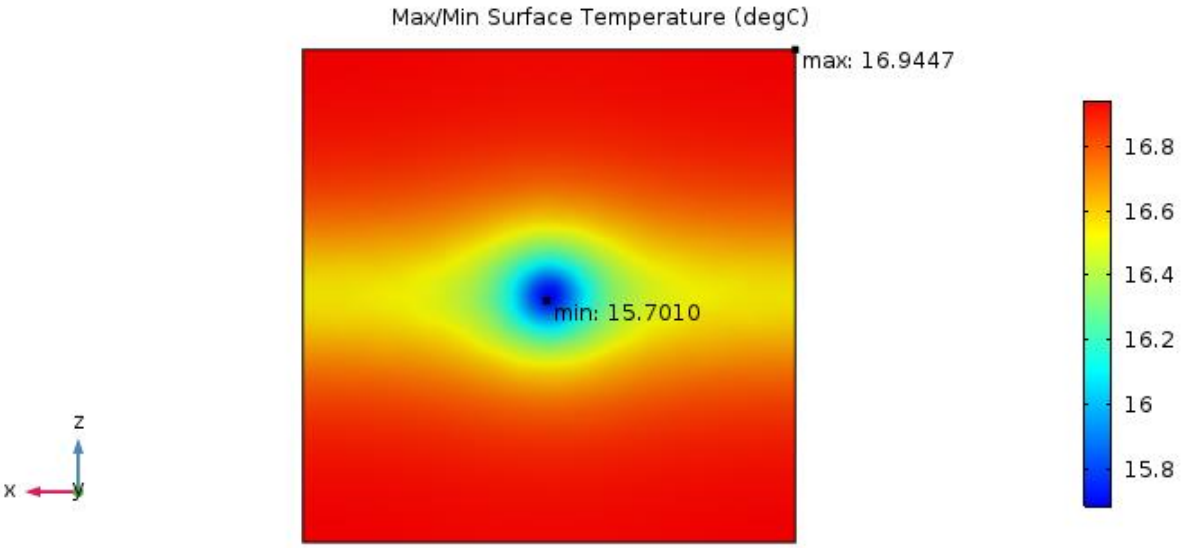

Figure 72 - Internal surface temperature CLT160-D10

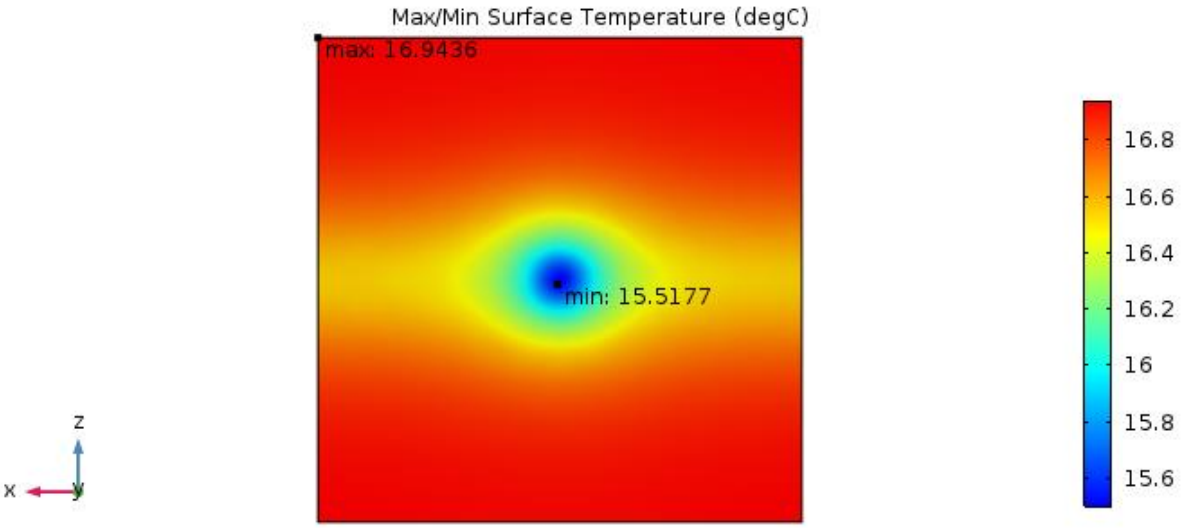

Figure 73 - Internal surface temperature CLT160-D12

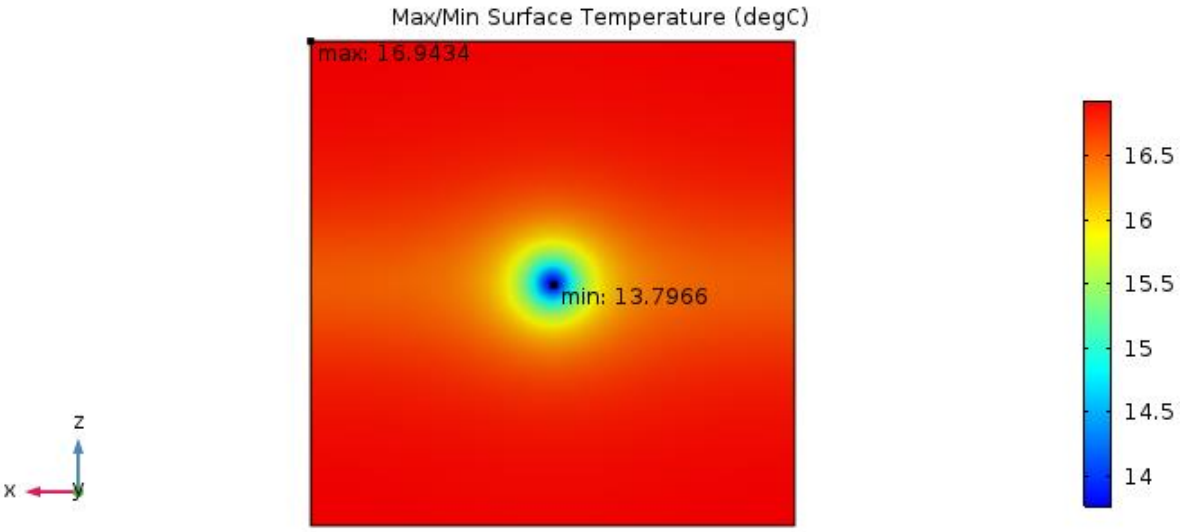

Figure 74 - Internal surface temperature CLT160-D16

Model type 3 x 4 m²

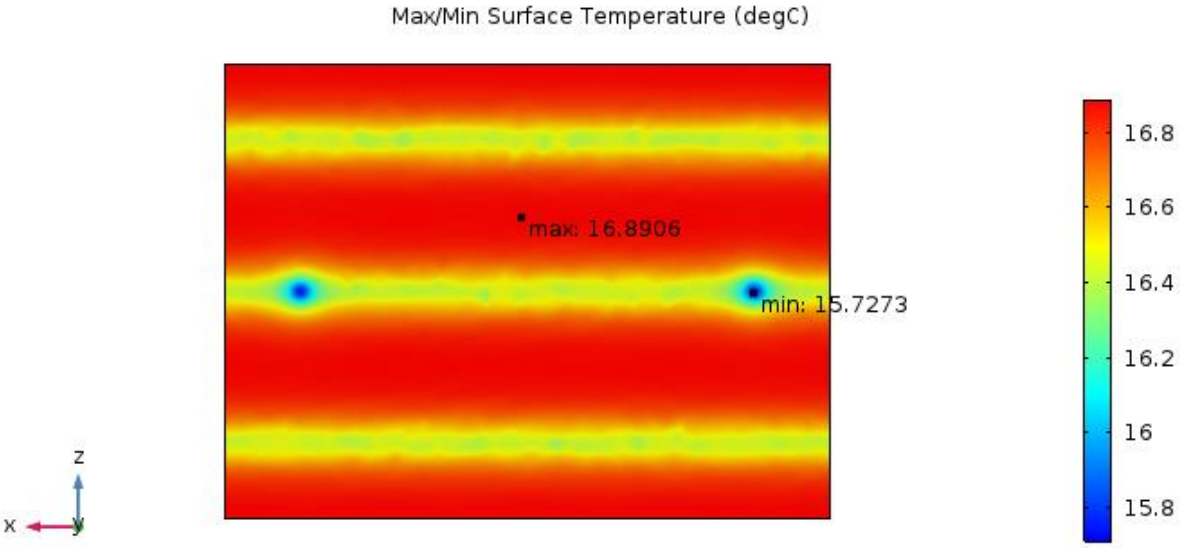

Figure 75 – Internal surface temperature CLT140-3x4-2D8

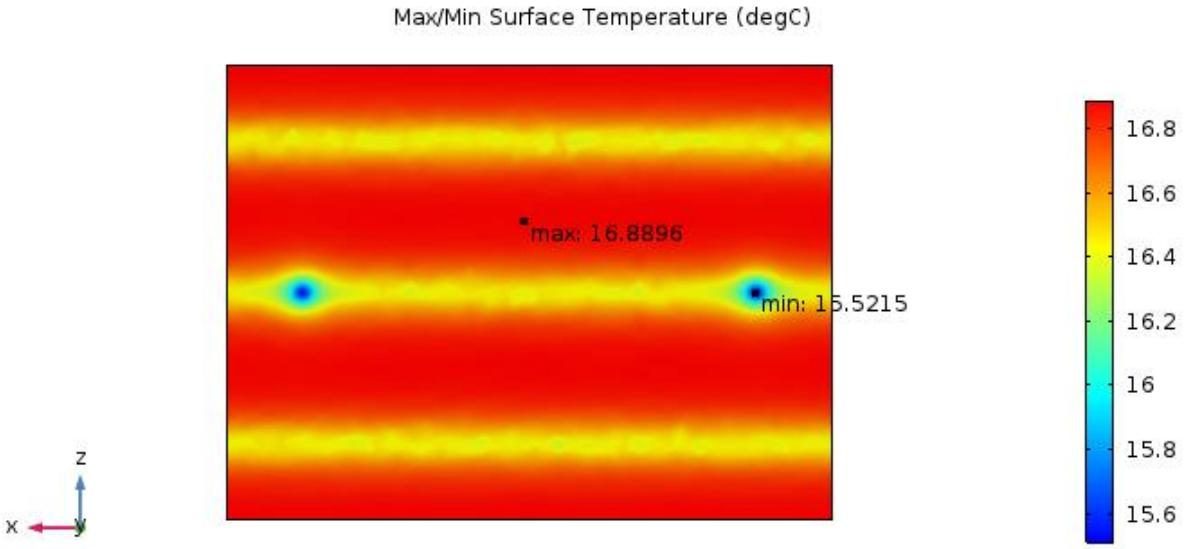

Figure 76 - Internal surface temperature CLT140-3x4-2D10

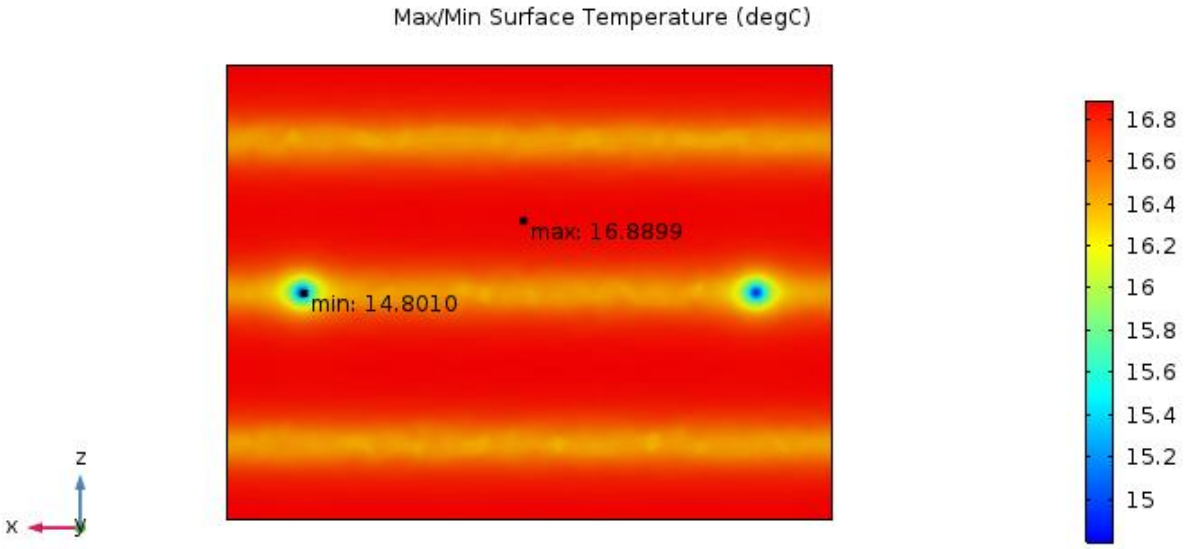

Figure 77 - Internal surface temperature CLT140-3x4-2D12

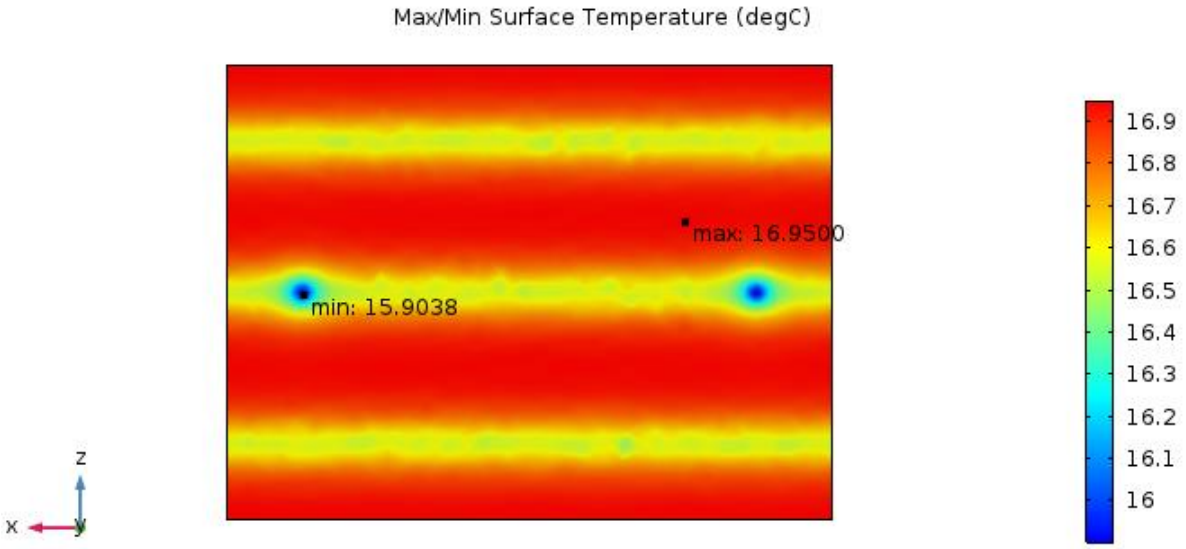

Figure 78 - Internal surface temperature CLT160-3x4-2D8

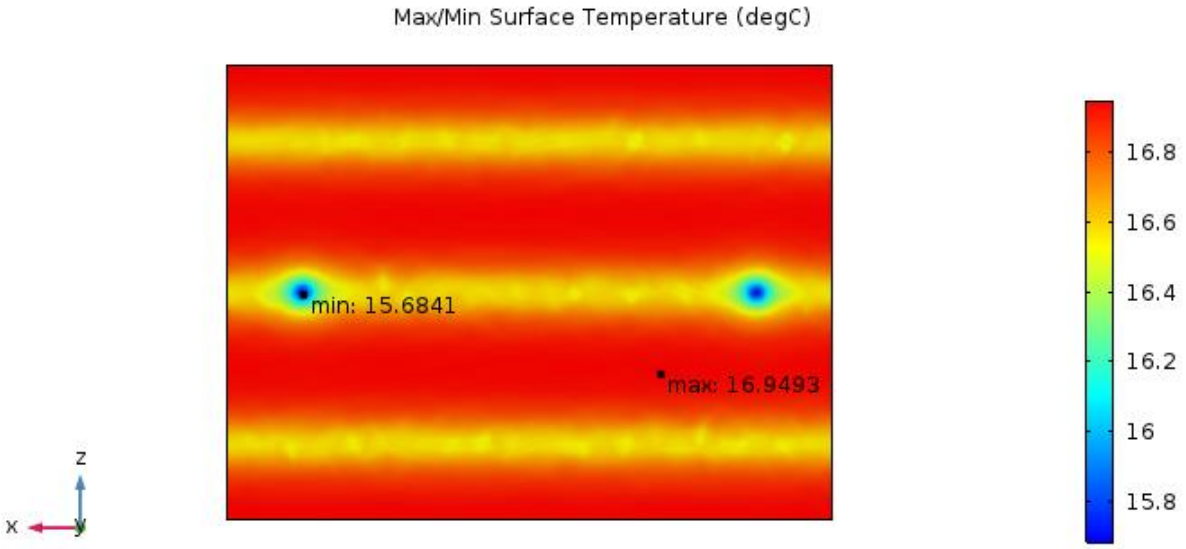

Figure 79 - Internal surface temperature CLT160-3x4-2D10

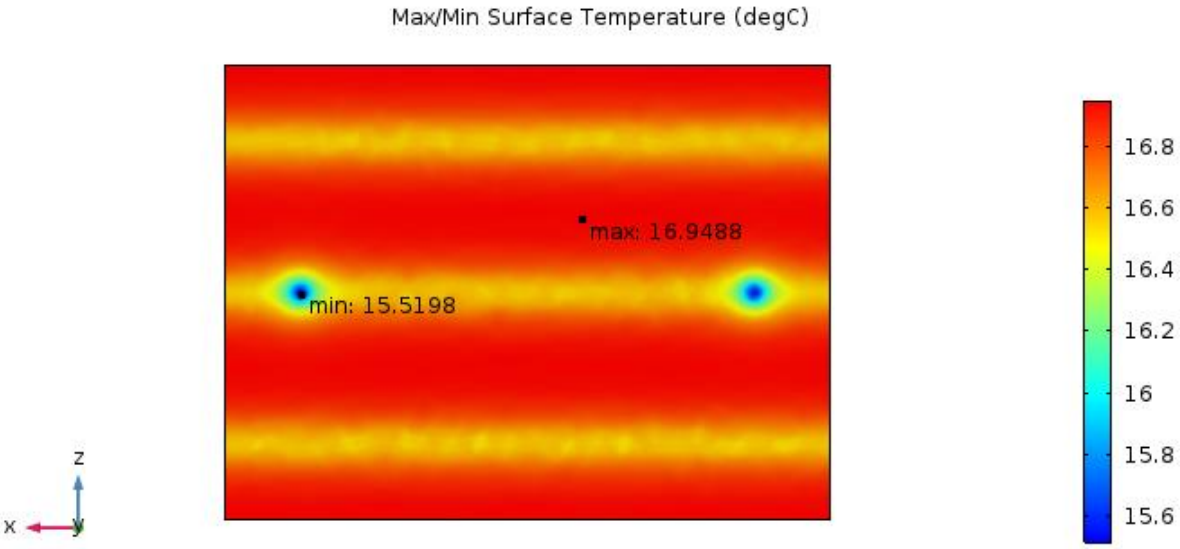

Figure 80 - Internal surface temperature CLT160-3x4-2D12

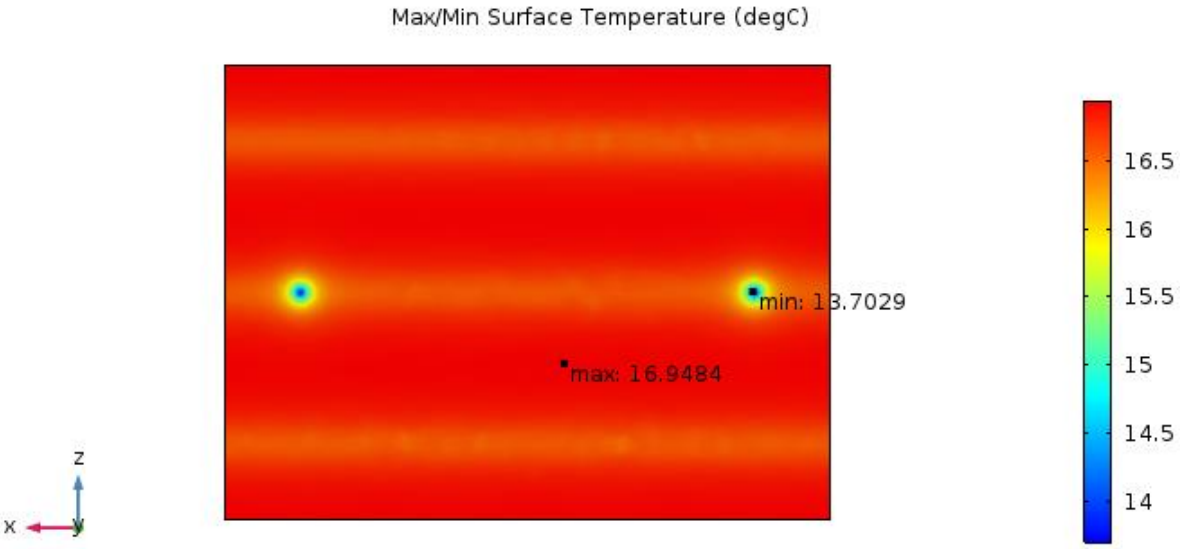

Figure 81 - Internal surface temperature CLT160-3x4-2D16

Model type floor/wall joint

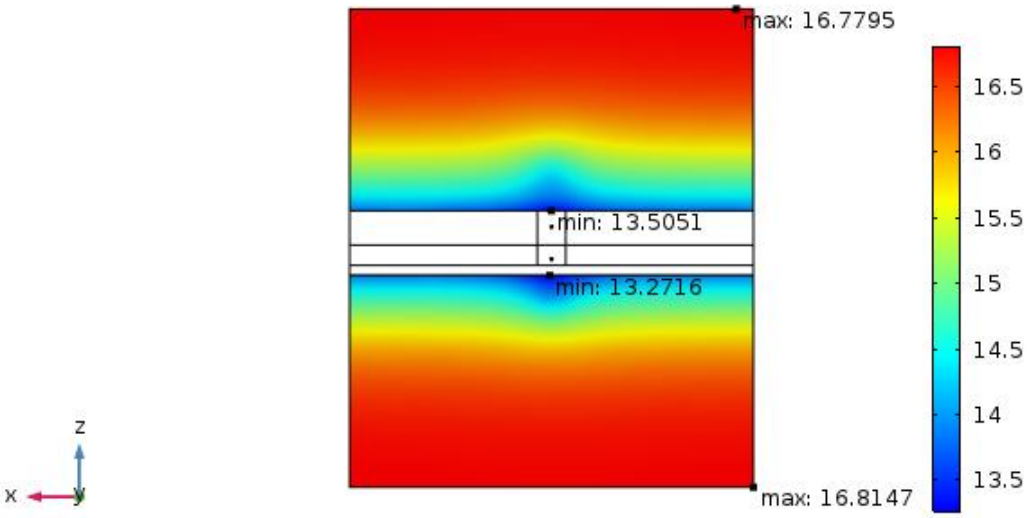

Figure 82 - Internal surface temperature F/W-barrier_CLT

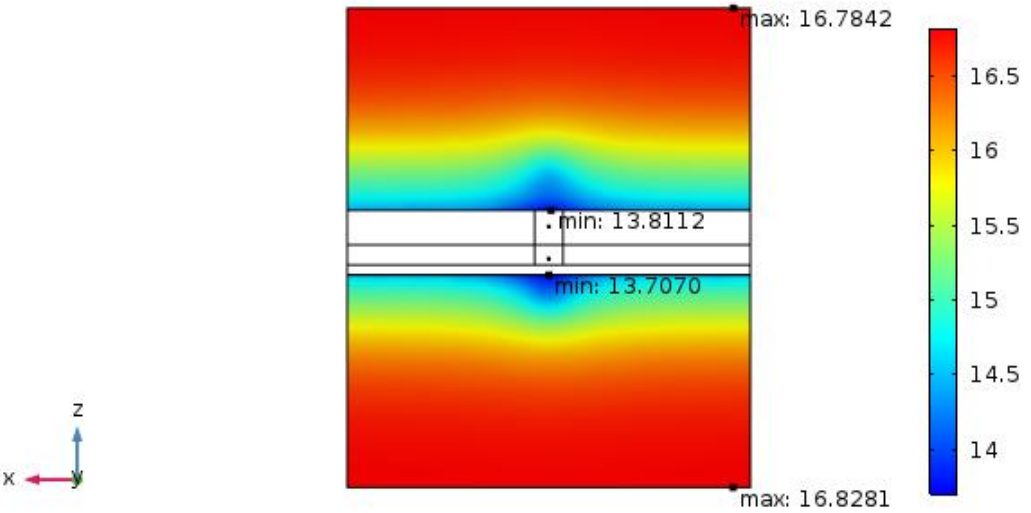

Figure 83 - Internal surface temperature F/W-barrier_ins

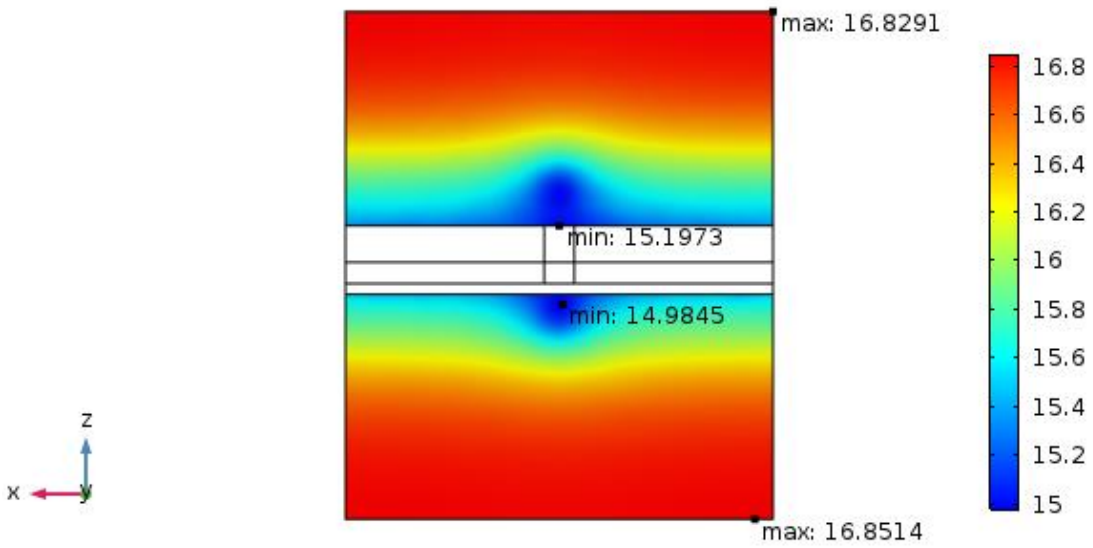

Figure 84 - Internal surface temperature F/W-no_barrier

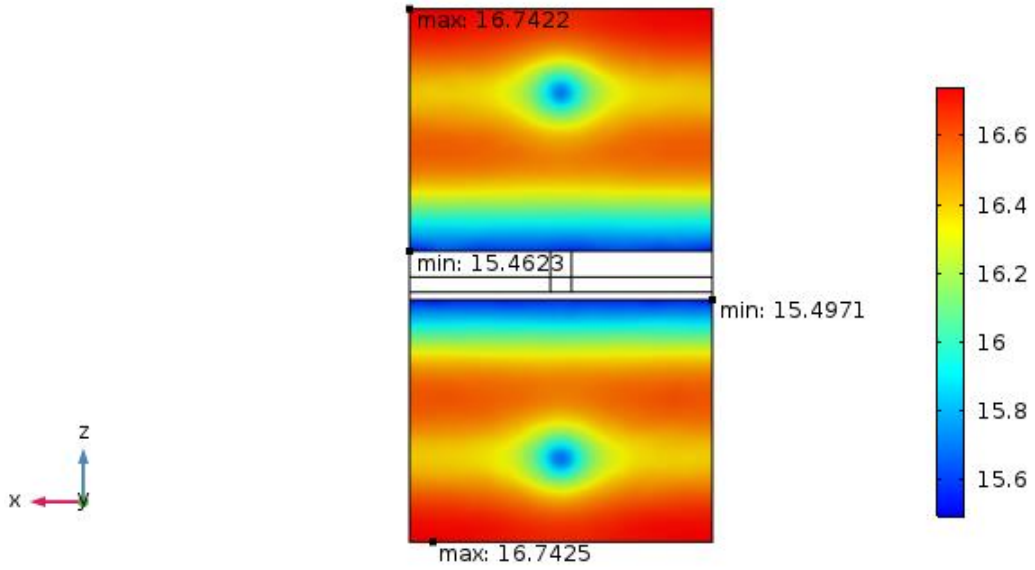

Figure 85 - Internal surface temperature F/W-conn_0.5

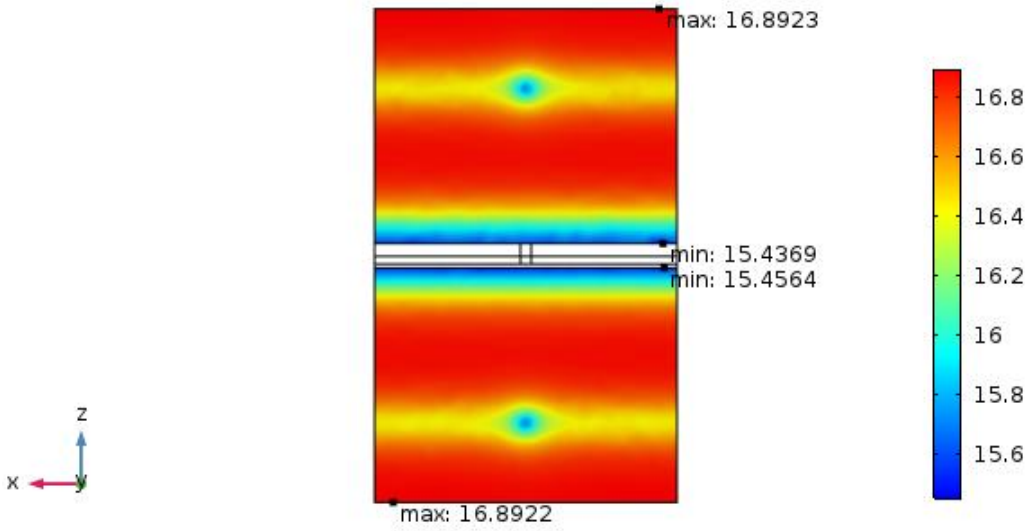

Figure 86 - Internal surface temperature F/W-conn_1.0

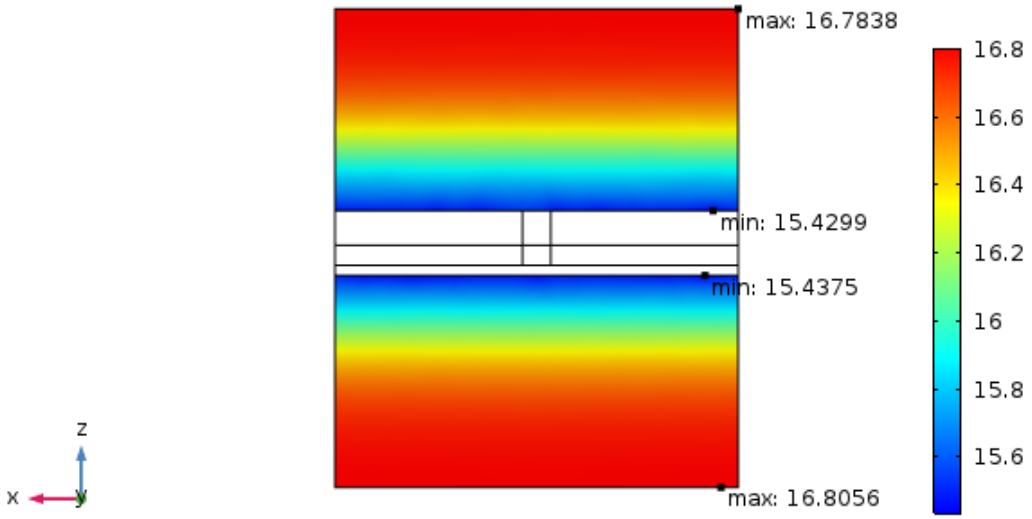

Figure 87 - Internal surface temperature F/W-no_conn

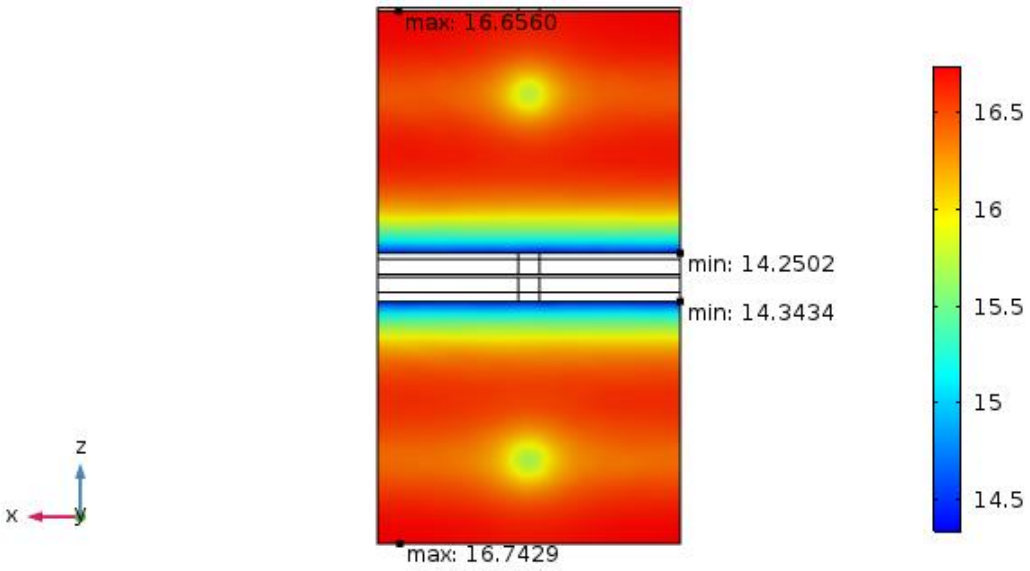

Figure 88 - Internal surface temperature F/W-diff